biomedicines

MDPI

Article

Structural Basis of the Interaction of the G Proteins, $G\alpha i_1$, $G\beta_1\gamma_2$ and $G\alpha i_1\beta_1\gamma_2$, with Membrane Microdomains and Their Relationship to Cell Localization and Activity

Rafael Álvarez [1,2] and Pablo V. Escribá [1,2,*]

[1] Department of Biology, University of the Balearic Islands, 07122 Palma, Spain
[2] Laminar Pharmaceuticals, 07122 Palma, Spain
* Correspondence: pablo.escriba@uib.es

Abstract: GPCRs receive signals from diverse messengers and activate G proteins that regulate downstream signaling effectors. Efficient signaling is achieved through the organization of these proteins in membranes. Thus, protein–lipid interactions play a critical role in bringing G proteins together in specific membrane microdomains with signaling partners. Significantly, the molecular basis underlying the membrane distribution of each G protein isoform, fundamental to fully understanding subsequent cell signaling, remains largely unclear. We used model membranes with lipid composition resembling different membrane microdomains, and monomeric, dimeric and trimeric Gi proteins with or without single and multiple mutations to investigate the structural bases of G protein–membrane interactions. We demonstrated that cationic amino acids in the N-terminal region of the $G\alpha i_1$ and C-terminal region of the $G\gamma_2$ subunit, as well as their myristoyl, palmitoyl and geranylgeranyl moieties, define the differential G protein form interactions with membranes containing different lipid classes (PC, PS, PE, SM, Cho) and the various microdomains they may form (Lo, Ld, PC bilayer, charged, etc.). These new findings in part explain the molecular basis underlying amphitropic protein translocation to membranes and localization to different membrane microdomains and the role of these interactions in cell signal propagation, pathophysiology and therapies targeted to lipid membranes.

Keywords: drug discovery; lipid rafts; membrane lipids; palmitoylation; protein structure; protein prenylation; lipid structure; protein–lipid interactions; membrane microdomain; cell signaling; membrane lipid therapy; melitherapy

Citation: Álvarez, R.; Escribá, P.V. Structural Basis of the Interaction of the G Proteins, $G\alpha i_1$, $G\beta_1\gamma_2$ and $G\alpha i_1\beta_1\gamma_2$, with Membrane Microdomains and Their Relationship to Cell Localization and Activity. *Biomedicines* **2023**, *11*, 557. https://doi.org/10.3390/biomedicines11020557

Academic Editors: Bart De Geest and Giulio Innamorati

Received: 3 January 2023
Revised: 1 February 2023
Accepted: 3 February 2023
Published: 14 February 2023

1. Introduction

The development of medicines targeting cell membranes requires a deep knowledge of the molecular basis that rule lipid bilayer structure and how this structure regulates signaling protein interactions with membranes and the ensuing cell signaling. Moreover, these interactions could be altered in association with pathophysiological processes and can be modulated by interventions with bioactive lipids and synthetic derivatives with therapeutic activity (membrane lipid therapy, melitherapy). The peripheral signaling proteins, G proteins, are composed of one α, β and γ subunits. There are currently known to be 18 different human Gα subunits, 6 different Gβ and 12 different Gγ subunits [1–4]. Activation of G proteins by agonist-activated G protein-coupled receptors (GPCRs) provokes the dissociation of the $G\alpha\beta\gamma$ heterotrimer into the Gα monomer and $G\beta\gamma$ dimer, each form regulating their respective effectors and other signaling proteins. In addition, Gα subunits can be modified at their N-terminus through the incorporation of myristic and/or palmitic acids, while γ subunits can be modified by the addition of farnesyl or geranylgeranyl moieties to their C-terminal cysteine; these modifications intervene in the interactions with membranes [1,5,6]. In this context, the abundant $G\alpha i_1\beta_1\gamma_2$ complex, an adenylyl cyclase

inhibitory (Gi) protein controlling cAMP levels, may contain one reversibly bound palmitoyl moiety as well as irreversibly bound myristoyl and geranylgeranyl moieties [7–9]. The aim of this study was to investigate the influences of membrane lipid structure and surface charge and the roles of G protein lipid modifications and charge on the interactions of G protein monomers ($G\alpha i_1$), dimers ($G\beta_1\gamma_2$) and trimers ($G\alpha i_1\beta_1\gamma_2$) with lipid membranes. The regulation of these protein–lipid interactions controls the localization of G proteins (and other amphitropic proteins) to different plasma membrane microdomains and organelles, where they may interact with distinct transmembrane and peripheral proteins, producing different signals [10]. The spatiotemporal organization of proteins forming signalosomes in defined membrane nano/microdomains is involved in many cellular processes [11,12]. Moreover, these signaling platforms formed in discrete membrane areas are relevant in pathological processes and their therapy [13].

The current view of the fluid mosaic model of the membrane [14] contemplates mosaicism in terms of a dynamically structured patchwork of membrane microdomains [15,16]. Under this new view of the fluid mosaic model, protein and lipid organization in the membrane follow a non-random co-distribution. Thus, proteins and lipids will form macromolecular structures or microdomains (small clusters of several nm or even μm) in conjunction with defined lipids and proteins in continuous dynamic turnover [15,17–19]. In this context, important changes in the membrane levels of one or more major lipids might be associated with the activation or deactivation of "lipid switches" that trigger or terminate crucial cellular processes, such as differentiation, cell proliferation, cell death, among others [20]. This fact further indicates the relevance of G protein–lipid interactions in human disease and therapy through approaches that control cell membrane lipid composition and structure. Lipid polymorphism (or lipid mesomorphism), the ability of lipids to form different stable or transient structures, is key to understanding how specific proteins interact with lipid bilayers and how these membrane microdomains regulate and are regulated by protein–lipid interactions [16,17,21–23]. Thus, lipids with a bulky polar head that are similar to cylinders (e.g., phosphatidylcholine—PC) give rise to lamellar structures, of which liquid ordered membrane microdomains (Lo) have been widely studied. Several classes of Lo membrane microdomains have been described, which are usually rich in sphingomyelin (SM) and cholesterol (Cho), and they have been termed *lipid rafts*. However, a variety of detergent-resistant microdomains may display specific features according to the presence and levels of caveolins, gangliosides, Cho, among others. By contrast, lipids with a small polar head (e.g., phosphatidylethanolamine [PE], diacylglycerol [DAG]) would be prone to form non-lamellar structures, such as inverted hexagonal phases (H_{II}), and these are abundant in liquid disordered (Ld) lipid bilayer microdomains. The behavior of lipids in vitro reflects the membrane nano/microdomains that they form, which defines the location of important lipidated signaling proteins, such as G proteins [24]. The nature of the lipids covalently bound to these membrane proteins is also crucial. Thus, acylated proteins prefer raft-like liquid-ordered (Lo) domains while prenylated proteins are excluded from these membrane regions and prefer non-lamellar prone [24–27]. Moreover, the small G protein, KRAS, interacts preferably with membrane microdomains rich in negatively charged phospholipids (e.g., phosphatidylserine—PS), its isoprenyl moiety and positively charged C-terminal amino acids participating in the modulation of this binding with different PS nanodomains [28].

The movement of lipids and proteins in biological membranes is strongly regulated by the highly ordered *lipid rafts* [29,30]. Large unilamellar vesicles (LUVs) composed of equimolar quantities of PC, PE, Cho and SM can form raft-like microdomains with a high Cho and SM content, as in [31], wherein these were used as model rafts. PS is another important lipid, and it is predominantly localized to the inner monolayer of the plasma membrane [32] where it plays an important regulatory role [33–35]. Here, we demonstrated the existence of key interactions between the C-terminal polybasic domain of $G\gamma_2$ and PS in the binding of $G\beta_1\gamma_2$ and $G\alpha i_1\beta_1\gamma_2$ to PS membranes. Moreover, we showed here that changes caused by reversible G protein palmitoylation influence the affinity for these

charged microdomains. Interestingly, the present study reveals that G protein lipid anchors are crucial in the synergistic preference of heterodimers and heterotrimers with different lipid modifications for charged and non-lamellar prone membrane microdomains, which in part explains the affinity of peripheral protein peptides for PS-rich nanodomains [28]. In addition, each G protein subunit amino acid studied here plays a specific role in its binding to the lipid bilayer and later in its sorting to defined membrane microdomains. This extends previous data from our group [6,23,24,35,36], providing new relevant information about the precise influence of G protein and membrane lipid structures in G protein–membrane interactions that go beyond specific interactions of membrane proteins with defined lipids (e.g., ghrelin receptor and PIP2, [37]). Finally, the knowledge gained in this field can be used to design biomedicines to treat numerous conditions in which protein–lipid interactions are involved in pathophysiological cell signaling [38,39].

2. Materials and Methods

2.1. Materials

The pFastBac 1 vector was purchased from Invitrogen (Barcelona, Spain). Miller's LB Broth culture medium and agarose D-1 were obtained from Conda Laboratories (Barcelona, Spain), while Grace's medium was from GIBCO (Madrid, Spain). Penicillin and streptomycin were purchased from PAA (Pasching, Austria) and β-Mercaptoethanol from Acros Organics (Madrid, Spain). CHAPS was supplied by AppliChem (Darmstadt, Germany). The antibodies against $G\alpha i_1$ (clone R4), $G\beta_1$ (ref. sc-379) and $G\gamma_2$ (ref. sc-374) were obtained from Santa Cruz Biotechnology (Santa Cruz, CA, USA). IRDye 800CW-linked donkey anti-mouse IgG and IRDye 800CW-linked donkey anti-rabbit IgG were provided by Li-Cor Biosciences (Madrid, Spain). Palmitoyl-CoA, egg-PC, liver-PE, egg-SM, porcine brain-PS (phosphatidylserine) and Cho were obtained from Avanti Polar Lipids (Alabaster, AL, USA). The natural phospholipids used had a balanced proportion of saturated and unsaturated acyl chains, mainly palmitic, stearic, oleic, linoleic and arachidonic acids. Brain PS showed high levels of docosahexaenoic acid (DHA, 11%) and the main fatty acid found in egg SM was palmitic acid (86%). For further details, see the manufacturer's website. GDP, GDPβS, HEPES, Tris-HCl, proteinase inhibitors and all other reagents were purchased from Sigma-Aldrich (Madrid, Spain).

2.2. Site-Directed Mutagenesis and Cloning of G Proteins

The cDNA encoding the recombinant $G\alpha i_1$ protein was kindly provided in the pQE-60 expression vector (3.4 kb) by Prof. Alfred G. Gilman (University of Texas Southwestern Medical Center, Dallas). The cDNA encoding the human $G\gamma_2$ protein was generously provided by Dr Scott Gibson (Southwestern Medical School, University of Texas) and the amino acid sequence of this protein is shown in Table 1. Site-directed mutagenesis of the $G\alpha i_1$ and $G\gamma_2$ proteins were carried out as described elsewhere [35], and in the case of the latter, it was performed using the primers shown in Table 2. The amino acid sequence and modifications of $G\alpha i_1$ are shown elsewhere [35]. Finally, the cDNA encoding the human $G\beta_1$ protein was a gift from Drs. Lutz and Niroomand (University of Heidelberg, Germany). The $G\alpha i_1$, $G\beta_1$ and $G\gamma_2$ cDNAs were cloned into the pFastBac 1 expression vector as described previously [35] and combined to produce the G protein monomers, dimers and trimers used in the present study (e.g., Figures S1–S3).

Table 1. Amino acid sequence of the recombinant human $G\gamma_2$ protein.

H2N-MASNNTASIAQARKLVEQLKMEANIDRIKVSKAAADLMAYCEAHAKEDPLL TPVPASENPFREKKFFCAIL-COOH

Table 2. PCR primers used and their corresponding amino acid sequences.

Proteins	Forward Oligonucleotide
	5′-ATC**GAATTC**ATGGCCAGCAACAACACCGCCAGCATAGCACAAGCCAG-3′
	Reverse Oligonucleotides
wild type $G\gamma_2$	5′-CTC**GCGGCCGC**TTAAAGGATAGCACAGAA-3′
GER- $G\gamma_2$	5′-CTC**GCGGCCGC**TTAAAGGATAGCAGAGAA-3′
R62G $G\gamma_2$	5′-CTC**GCGGCCGC**TTAAAGGATAGCACAGAAAAACTTCTTCTCCCCAAA-3′
K64G $G\gamma_2$	5′-CTC**GCGGCCGC**TTAAAGGATAGCACAGAAAAACTTCCCTCCCTAAA-3′
K65G $G\gamma_2$	5′-CTC**GCGGCCGC**TTAAAGGATAGCACAGAAAAACCCTTCTCCCTAAA-3′
R62G K64G $G\gamma_2$	5′-CTC**GCGGCCGC**TTAAAGGATAGCACAGAAAAACTTCCCTCCCCAAA-3′
R62G K65G $G\gamma_2$	5′-CTC**GCGGCCGC**TTAAAGGATAGCACAGAAAAACCCTTCTCCCCAAA-3′
K64G K65G $G\gamma_2$	5′-CTC**GCGGCCGC**TTAAAGGATAGCACAGAAAAACCCCCCTCCCTAAA-3′
R62G K64G K65G $G\gamma_2$	5′-CTC**GCGGCCGC**TTAAAGGATAGCACAGAAAAACCCCCCTCCCCAAA-3′
GER-R62G $G\gamma_2$	5′-CTC**GCGGCCGC**TTAAAGGATAGCAGAGAAAAACTTCTTCTCCCCAAA-3′
GER-K64G $G\gamma_2$	5′-CTC**GCGGCCG**CTTAAAGGATAGCAGAGAAAAACTTCCCTCCCTAAA-3′
GER-K65G $G\gamma_2$	5′-CTC**GCGGCCGC**TTAAAGGATAGCAGAGAAAAACCCTTCTCCCTAAA-3′
GER-R62G K64G $G\gamma_2$	5′-CTC**GCGGCCGC**TTAAAGGATAGCAGAGAAAAACTTCCCTCCCCAAA-3′
GER-R62G K65G $G\gamma_2$	5′-CTC**GCGGCCGC**TTAAAGGATAGCAGAGAAAAACCCTTCTCCCCAAA-3′
GER-K64G K65G $G\gamma_2$	5′-CTC**GCGGCCG**CTTAAAGGATAGCAGAGAAAAACCCCCCTCCCTAAA-3′
GER-R62G K64G K65G $G\gamma_2$	5′-CTC**GCGGCCGC**TTAAAGGATAGCAGAGAAAAACCCCCCTCCCCAAA-3′

2.3. G Protein Purification

2.3.1. $G\alpha i_1$ Proteins

Recombinant wild type and mutant $G\alpha i_1$ proteins were overexpressed and purified using affinity chromatography as described previously [35]. Briefly, the recombinant proteins were expressed in Sf9 cells using the Bac-to-Bac Baculovirus Expression System (Invitrogen). Then, recombinant $G\alpha i_1$ proteins were produced in Sf9 cells, which were cultured in suspension in Grace's medium supplemented with 10% FCS (v/v), penicillin (100 units/mL) and streptomycin (100 µg/mL). The WT and Pal–$G\alpha i_1$ subunits were purified from Sf9 cell membrane fractions after harvesting Sf9 cells by centrifugation and suspending them in 15 mL of ice-cold 20 mM HEPES buffer (pH 8.0) containing β-mercaptoethanol (10 mM), NaCl (100 mM), MgCl2 (1 mM), GDP (10 µM) and proteinase inhibitors (lysis buffer). The nuclei and unbroken cells were removed by centrifugation at 3000× g for 10 min at 4 °C, and the resulting sample was centrifuged again at 100,000× g for 1 h at 4 °C. The membranes recovered were suspended in 6 mL of HEPES buffer (50 mM, pH 8.0) containing β-mercaptoethanol (10 mM), NaCl (500 mM), CHAPS (16 mM), GDP (10 µM) and proteinase inhibitors, and after incubating for 1 h with gentle shaking, the membranes were centrifuged at 100,000× g for 1 h. The resulting supernatant (membrane extract) was dialyzed against HEPES buffer supplemented with GDP (0.5 µM) and leupeptin (50 ng/mL) and then purified by chromatography on a Ni-NTA column (1 mL of resin, Invitrogen). Subsequently, the resin was washed with 30 mL of HEPES buffer (20 mM, pH 8.0) containing β-mercaptoethanol (10 mM), NaCl (400 mM), C12E10 (0.05%, v/v), GDP (10 µM), leupeptin (0.5 µg/mL) and imidazole (15 mM), using an increasing and discontinuous thermal gradient (4, 17 and 25 °C). The column was then washed with 20 mL of HEPES buffer (20 mM, pH 8.0) containing MgCl2 (0.5 mM), β-mercaptoethanol (10 mM), NaCl (100 mM), C12E10 (0.05%, v/v), GDP (10 µM), leupeptin (0.5 µg/mL) and imidazole (15 mM) at 30 °C, and it was then activated with 10 mL of HEPES buffer (20 mM, pH 8.0) containing AlCl3 (30 µM), MgCl2 (50 mM) and NaF (10 mM, AMF buffer). Finally, the $G\alpha i_1$ protein was eluted with HEPES buffer (20 mM, pH 8.0) containing β-mercaptoethanol (10 mM), NaCl (100 mM) and MgCl2 (1 mM, elution buffer) and was supplemented with a step gradient of imidazole (40, 80, 120, 240 and 300 mM). The purified protein was dialyzed and stored at −80 °C until use. The Myr–$G\alpha i_1$ mutant protein was overexpressed and purified from the cytosolic fraction of infected Sf9 cells, which had been harvested and suspended in 5 mL

of ice-cold lysis buffer as indicated above. The Myr–Gαi_1 protein was purified from the supernatant by affinity chromatography as indicated above and fractionated by SDS-PAGE followed by coomassie blue staining.

2.3.2. G$\beta_1\gamma_2$ Dimers

G$\beta_1\gamma_2$ complexes were purified as described previously [40] with some modifications. Briefly, Sf9 cells were co-infected with a recombinant baculovirus encoding wild type (WT) Gβ_1 and Gγ_2 (WT or mutant) subunits. Heterodimers were purified after harvesting Sf9 cells by centrifugation and resuspending them in ice-cold 50 mM HEPES buffer (pH 8.0) containing 10 mM β-mercaptoethanol, 500 mM NaCl, 10 µM GDP and proteinase inhibitors (lysis buffer). After cell nitrogen cavitation lysis at 500 p.s.i. for 30 min (Parr pump, [40]), nuclei and unbroken cells were removed by centrifugation at 3000× *g* for 10 min at 4 °C. Subsequently, 16 mM CHAPS was added to the sample and the resulting homogenate (10 mL) was shaken gently for 1 h at 4 °C and finally, it was centrifuged at 100,000× *g* for 1 h. The supernatant recovered was dialyzed against HEPES buffer containing 100 mM NaCl, 0.5 µM GDP and 50 ng/mL leupeptin, and the GDP concentration was then increased to 1 mM before the G$\beta_1\gamma_2$ dimers were purified by chromatography on a Ni-NTA column (0.5 mL of resin with a maximum binding capacity of 2.5–5 mg protein: Invitrogen). The resin was washed with 20 mL of 20 mM HEPES buffer (pH 8.0) containing 10 mM β-mercaptoethanol, 400 mM NaCl, 0.05% C12E10 (*v*/*v*), 1 mM GDP and 0.5 µg/mL leupeptin, following an increasing and discontinuous thermal gradient (4, 17 and 25 °C). The column was then washed with 5 mL of 20 mM HEPES buffer (pH 8.0) containing 10 mM β-mercaptoethanol, 100 mM NaCl, 0.05% C12E10 (*v*/*v*), 1 mM GDP, 0.5 µg/mL leupeptin and 5 mM imidazole at 25 °C and with 20 mL of the same buffer at 30 °C. G$\beta\gamma$ dimers were eluted from the column using 15 mL of 20 mM HEPES buffer (pH 8.0) with 30 µM AlCl3, 50 mM MgCl2 and 10 mM NaF (AMF buffer), and the purified dimers were dialyzed and stored at −80 °C until use.

2.3.3. G$\alpha i_1\beta_1\gamma_2$ Heterotrimers

Purified Gαi_1 monomers (WT, Pal– and Myr– Gαi_1) and G$\beta_1\gamma_2$ dimers (WT and RKK G$\beta_1\gamma_2$) were combined in a 1:1.5 ratio (*w*:*w*), and the different samples were then lyophilized. The dry residue was suspended in water in the presence of 5 mM GDPβS and incubated at 30 °C for 30 min. The samples were then diluted in 20 mM HEPES buffer (pH 8.0) containing 0.4 mM DTT, 100 mM KCl, 0.05% C12E10 (*v*/*v*) and 0.5 mM GDP. The samples were shaken overnight at 4 °C. Each protein mixture was combined with an Ni-NTA resin and then centrifuged at 800× *g* for 2 min at 4 °C, and the pellets recovered were washed with 500 µL of 20 mM HEPES buffer (pH 8.0) containing 0.4 mM DTT, 100 mM KCl, 0.005% C12E10 (*v*/*v*) and 0.5 mM GDP. After four washes, the proteins to the affinity resin were eluted with 450 µL (3 × 150 µL) of 20 mM HEPES buffer (pH 8.0) containing 0.4 mM DTT, 100 mM KCl, 0.005% C12E10 (*v*/*v*), 0.5 mM GDP and 300 mM imidazole. The G$\alpha i_1\beta_1\gamma_2$ complexes recovered were diluted in 20 mM HEPES buffer (pH 8.0) containing 1 mM DTT, 100 mM KCl, 1 mM EDTA and 50 µM GDP and desalted and concentrated using Amicon centrifugal filters with a molecular weight cut-off of 50 kDa (Millipore). Concentrated G$\alpha i_1\beta_1\gamma_2$ heterotrimers were frozen in liquid nitrogen and stored at −80 °C until use (Figures S1–S6).

2.4. Acylation Reaction in G$\alpha i_1\beta_1\gamma_2$ Heterotrimers

Purified G$\alpha i_1\beta_1\gamma_2$ heterotrimers containing a myristoylated WT Gαi_1 protein were subjected to in vitro palmitoylation as described elsewhere [27,35] with some modifications. Briefly, heterotrimers (0.1–0.3 nmol) were incubated with 20 nmol of palmitoyl-CoA for 3 h at 30 °C in 1 mL of 20 mM HEPES buffer containing 2 mM MgCl2, 50 mM NaCl, 1 mM EDTA, 0.2 mM DTT, 0.5 µM GDP and 7.5 mM CHAPS (pH 7.6). The heterotrimers were then diluted in HEPES buffer (20 mM, pH 8.0), containing DTT (0.2 mM), KCl (100 mM), EDTA

(1 mM) and GDP (50 µM) and concentrated using Amicon centrifugal filters of 50 kDa, as described above. Finally, the resulting complexes were stored at −80 °C until use.

2.5. G Protein Binding to Model Membranes

Model membranes (liposomes) were prepared as described elsewhere [35,36], and liposomes (1 mM) were incubated for 1 h at 25 °C with 150 ng of purified monomer, 100 ng of dimers or 50 ng of heterotrimers in a total volume of 300 µL. Unbound G proteins were then separated from the membrane-bound G proteins by centrifugation at 90,000× *g* for 1 h at 25 °C. Finally, membrane pellets were resuspended in 36 µL of 80 mM Tris-HCl buffer [pH 6.8], containing 4% SDS, and mixed with 4 µL of 10× electrophoresis loading buffer (120 mM Tris HCl (pH 6.8), 1.43 M β-mercaptoethanol, 2% SDS and 50% glycerol).

The binding of the different $G\alpha i_1$ monomers and $G\beta_1\gamma_2$ dimers to membranes were performed and quantified similarly as described [35]. Briefly, proteins were submitted to electrophoresis on 10% polyacrylamide gels and then transferred to nitrocellulose membranes. In these assays, a 1:200 dilution of anti-$G\beta_1$ was used to detect the $G\beta_1$ protein in the dimers in both the pellet and supernatant fractions. The membranes were finally incubated at room temperature for 1 h with IRDye 800CW-linked donkey anti-mouse IgG (1:5000 diluted in blocking solution), and antibody binding was detected by near infrared fluorescence using an ODYSSEY near infrared radiation detection system (LI-COR Biosciences).

Binding of $G\alpha i_1\beta_1\gamma_2$ heterotrimers to membranes was quantified as described elsewhere [24]. Briefly, the membranes were probed with the specific anti-$G\alpha i_1$ (dilution 1:100) and anti-$G\beta_1$ (dilution 1:200) antibodies in blocking solution, and the binding of these antibodies was detected with horseradish peroxidase-linked anti-mouse and anti-rabbit secondary antibodies, respectively. The signal was developed with the ECL Western blot detection system and ECL Hyperfilm (Amersham).

2.6. G Protein Structure Analysis

Protein sequences were obtained from the protein database record at the National Center for Biotechnology Information (http://www.ncbi.nlm.nih.gov accessed on 9 March 2010). The sequence identification numbers assigned by the International Nucleotide Sequence Database Collaboration to the different considered Gγ proteins are (Table 3): AAH29367.1 ($G\gamma_1$), AF493870.1 ($G\gamma_2$), AAH15563.1 ($G\gamma_3$), AAH22485.1 ($G\gamma_4$), AAH03563.1 ($G\gamma_5$), AAH53630.1 ($G\gamma_7$), AAH95514.1 ($G\gamma_8$), AAM12590.1 ($G\gamma_9$), AAH10384.1 ($G\gamma_{10}$), AAH09709 ($G\gamma_{11}$), AAM12593.1 ($G\gamma_{12}$) and AAH93760.1 ($G\gamma_{13}$). The secondary structure prediction of these Gγ proteins was performed on the Psi-Pred server using the default parameter settings. The sequences of these Gγ proteins were aligned with the CLUSTAL W (1.81) tool on the Biology WorkBench Interface (v. 3.2) as described elsewhere [35]. A bi-dimensional projection of the hypothetical C-terminal α helix of the $G\gamma_2$ protein was obtained with the HELIQUEST server, and in this projection, the one-letter code size was proportional to the amino acid volume.

Table 3. Multiple sequence alignment of human Gγ proteins.

-MPVINIEDLTEKDKLKMEVDQLKKEVTLERMLVSKCCEEVRDYVEERSGEDPLVKGIPEDKNPFKELKGGCVIS	Gγ1
—-MASN–NTASIAQARKLVEQLKMEANIDRIKVSKAAADLMAYCEAHAKEDPLLTPVPASENPFREKKFFCAIL	Gγ2
MKGETPVN–STMSIGQARKMVEQLKIEASLCRIKVSKAAADLMTYCDAHACEDPLITPVPTSENPFREKKFFCALL	Gγ3
KEGMSNN–STTSISQARKAVEQLKMEACMDRVKVSQAAADLLAYCEAHVREDPLIIPVPASENPFREKKFFCTIL	Gγ4
—-MS—-GSSSVAAMKKVVQQLRLEAGLNRVKVSQAAADLKQFCLQNAQHDPLLTGVSSSTNPFRPQKV-CSFL	Gγ5
—-MS—-ATNNIAQARKLVEQLRIEAGIERIKVSKAASDLMSYCEQHARNDPLLVGVPASENPFKDKKP-CIIL	Gγ6
—-MS-N–NMAKIAEARKTVEQLKLEVNIDRMKVSQAAAELLAFCETHAKDDPLVTPVPAAENPFRDKRLFCVLL	Gγ7
———-MAQDLSEKDLLKMEVEQLKKEVKNTRIPISKAGKEIKEYVEAQAGNDPFLKGIPEDKNPFKE-KGGCLIS	Gγ8
—-MS—-SGASASALQRLVEQLKLEAGVERIKVSQAAAELQQYCMQNACKDALLVGVPAGSNPFREPRS-CALL	Gγ9
—MPALHIEDLPEKEKLKMEVEQLRKEVKLQRQQVSKCSEEIKNYIEERSGEDPLVKGIPEDKNPFKE-KGSCVIS	Gγ10
—-MSSKTASTNNIAQARRTVQQLRLEASIERIKVSKASADLMSYCEEHARSDPLLIGIPTSENPFKDKKT-CIIL	Gγ12
———MEEWDVPQMKKEVESLKYQLAFQREMASKTIPELLKWIEDGIPKDPFLNPDLMKNNPWVE-KGKCTIL	Gγ13

The different human Gβ proteins were aligned using the CLUSTAL W (1.81) tool previously described, considering the Gβ proteins: AAM15918.1 ($G\beta_1$), AAM15919.1 ($G\beta_2$), AAM15920.1 ($G\beta_3$), AAG18442.1 ($G\beta_4$) and AAH13997.1 ($G\beta_5$). The three-dimensional structure of the $G\alpha i_1\beta_1\gamma_2$ heterotrimer (identifier number 49238 in the Molecular Modeling Database, MMDB) was displayed using the Cn3D 4.3 macromolecular structure viewer. Anionic and cationic amino acids in the trimer were detected and highlighted using this computer application.

Multiple alignment of all the known human Gγ proteins obtained with *CLUSTAL W (1.81)*. The last 23 amino acids of $G\gamma_2$ are highlighted, in particular, the C-terminal basic amino acids that are relevant to the protein–lipid interactions.

2.7. Data Analysis

The Origin software was used to analyze the data and perform the statistical analysis. Unless otherwise indicated, the results are expressed as the mean ± SEM values from at least three independent experiments. For G protein heterotrimers, protein–lipid interactions were measured using both anti-$G\alpha i_1$ and anti-$G\beta_1$ antibodies. Differences were considered statistically significant at $p < 0.05$. For the correlation analysis between the number of C atoms in the lipid anchors of amphitropic membrane proteins and the number of charged amino acids in their peptide-membrane interacting regions, a non-linear analysis with the seven groups of proteins indicated in Figure 10B was carried out using Origin to determine r, r^2 and χ^2.

3. Results

We have formerly investigated G protein–membrane interactions from different points of view and in the context of cell signaling, human pathophysiology and therapy [6,17,22–24,35,41–44]. The present study extends our previous investigations, providing a thorough report on the consequences of changes in relevant protein and lipid structural factors that drive the interaction of the three forms of G proteins, Gα monomers, Gβγ dimers and Gαβγ trimers, with model membranes that resemble different lipid microdomains. Thus, we have investigated the roles of both membrane lipid structure (phospholipid types, cholesterol content, surface charge, lateral pressure etc.) and G protein structure (lipidation and charge of the alpha and gamma subunits). In the present study, Myr- and Pal- mutants corresponded to the $G\alpha i_1$ subunit with the N-terminal G2A and C3S mutations that prevent protein myristoylation (Myr-) or palmitoylation (Pal-), respectively. Pal+ corresponded in the present study to the wild type $G\alpha i_1$ subunit, in which full protein palmitoylation was enzymatically achieved as described in the Materials and Methods Section 2. The basic C-terminal amino acids of the $G\gamma_2$ subunit, Arg-62, Lys-64 and Lys-65, were mutated to glycine (R62G, K64G and K65G, respectively) in single, double or triple mutants. In addition, the C68S mutation prevented the $G\gamma_2$ subunit geranylgeranylation and further processing (methylation and removal of the 3 C-terminal amino acids) [6], and it was studied in single or multiple mutants containing the above mutations. Finally, G protein heterotrimeric complexes of the wild type form and mutants of the alpha and/or gamma subunits (single or multiple combined mutations) were studied to define the role of these amino acids in the interactions with membranes. Altered protein–membrane interactions are associated with pathological processes and certain biomedicines, such as bioactive lipids, have been designed to treat relevant conditions.

3.1. Membranes Used in the Present Study

The plasma membrane is the preferred location for GPCR–G protein interactions. The most abundant phospholipid in this lipid bilayer is PC, which was used as a control to investigate the role of other membrane lipids on G protein–membrane interactions. *Lipid rafts* are L_o microdomains characterized by the abundance of SM and Cho, and they form spontaneously and segregate from L_d microdomains in PC:PE:SM:Cho (1:1:1:1, mole ratio) model membranes [45,46]. The intracellular leaflet of the plasma membrane has a high

proportion of PE and PS, phospholipids involved in the formation of Ld (non-lamellar prone) and of negatively charged membrane microdomains, respectively. These lipids were combined with PC to establish a model of microdomains that can be used to study G protein associations at the inner membrane leaflet.

3.2. The Role of $G\gamma_2$ C-Terminal Region in $G\beta_1\gamma_2$–Membrane Interactions

Hitherto, 12 different human Gγ subunits have been identified to date. These Gγ proteins were aligned, and the key amino acids that interact with membrane lipids are indicated in Table 3. The WT human $G\gamma_2$ protein and 15 mutated forms of this G protein subunit were transfected and overexpressed in Sf9 cells (Figure S1 and Table 4), and all the recombinant $G\gamma_2$ proteins produced were combined with the $G\beta_1$ protein, purifying the $G\beta_1\gamma_2$ complexes formed by affinity chromatography on a Ni-NTA column (see 'Materials and Methods' Section 2 and Figures S2 and S3). Single and multiple point mutations of the Arg-62, Lys-64, Lys-65 and Cys-68 amino acids in $G\gamma_2$ were induced, and the mutant and WT $G\beta_1\gamma_2$ dimers were studied (Table 4). Significantly, this latter Cys-68 (C68S) mutation impeded the geranylgeranylation of this $G\gamma_2$ subunit. In addition to the lack of one isoprenyl moiety at the C-terminal region of the C68G $G\gamma_2$ mutant, the last three amino acids were not removed and the peptide was not methylated at the C terminus [6]; all these alterations caused important changes in the physicochemical properties of the $G\gamma_2$ subunit site for membrane interactions (polarity and hydrophobicity). This may account for its different electrophoretic mobility compared to the wild type $G\gamma_2$ subunit. When all these dimers were analyzed independently and immunodetected with anti-$G\beta_1$ and anti-$G\gamma_2$ antibodies, the geranylgeranylated heterodimers had a similar electrophoretic mobility on non-denaturing polyacrylamide gels, which clearly differed from those of the non-geranylgeranylated counterparts (Figure S3).

Table 4. Site-directed mutagenesis of $G\gamma_2$.

WT	PLLTPVPASENPFREKKFFCAIL	PLLTPVPASENPFREKKFFSAIL	*ger-*
K65	PLLTPVPASENPFREKGFFCAIL	PLLTPVPASENPFREKGFFSAIL	*ger-K65*
K64	PLLTPVPASENPFREGKFFCAIL	PLLTPVPASENPFREGKFFSAIL	*ger-K64*
R62	PLLTPVPASENPFGEKKFFCAIL	PLLTPVPASENPFGEKKFFSAIL	*ger-R62*
K64K65	PLLTPVPASENPFREGGFFCAIL	PLLTPVPASENPFREGGFFSAIL	*ger-K64K65*
R62K65	PLLTPVPASENPFGEKGFFCAIL	PLLTPVPASENPFGEKGFFSAIL	*ger-R62K65*
R62K64	PLLTPVPASENPFGEGKFFCAIL	PLLTPVPASENPFGEGKFFSAIL	*ger-R62K64*
R62K64K65	PLLTPVPASENPFGEGGFFCAIL	PLLTPVPASENPFGEGGFFSAIL	*ger-R62K64K65*

The sequences of wild type $G\gamma_2$ and the mutants generated to include all the possible combinations of mutations of the key amino acids are shown. Key amino acids are shown in blue and the corresponding mutants are shown in black italic case.

3.2.1. Geranylgeranyl Is Critical for the Membrane Binding of $G\beta_1\gamma_2$

$G\beta_1\gamma_2$–membrane interaction assays were performed, in which the aforementioned WT and mutant $G\beta_1\gamma_2$ proteins were combined with model membranes that mimicked several membrane microdomains. The most outstanding effect was witnessed with the Gβγ C68S mutant. The membrane binding of the dimer that carried this mutation was drastically reduced for all the model membranes used in this study compared to those of isoprenylated $G\beta_1\gamma_2$ dimers (Figure 1).

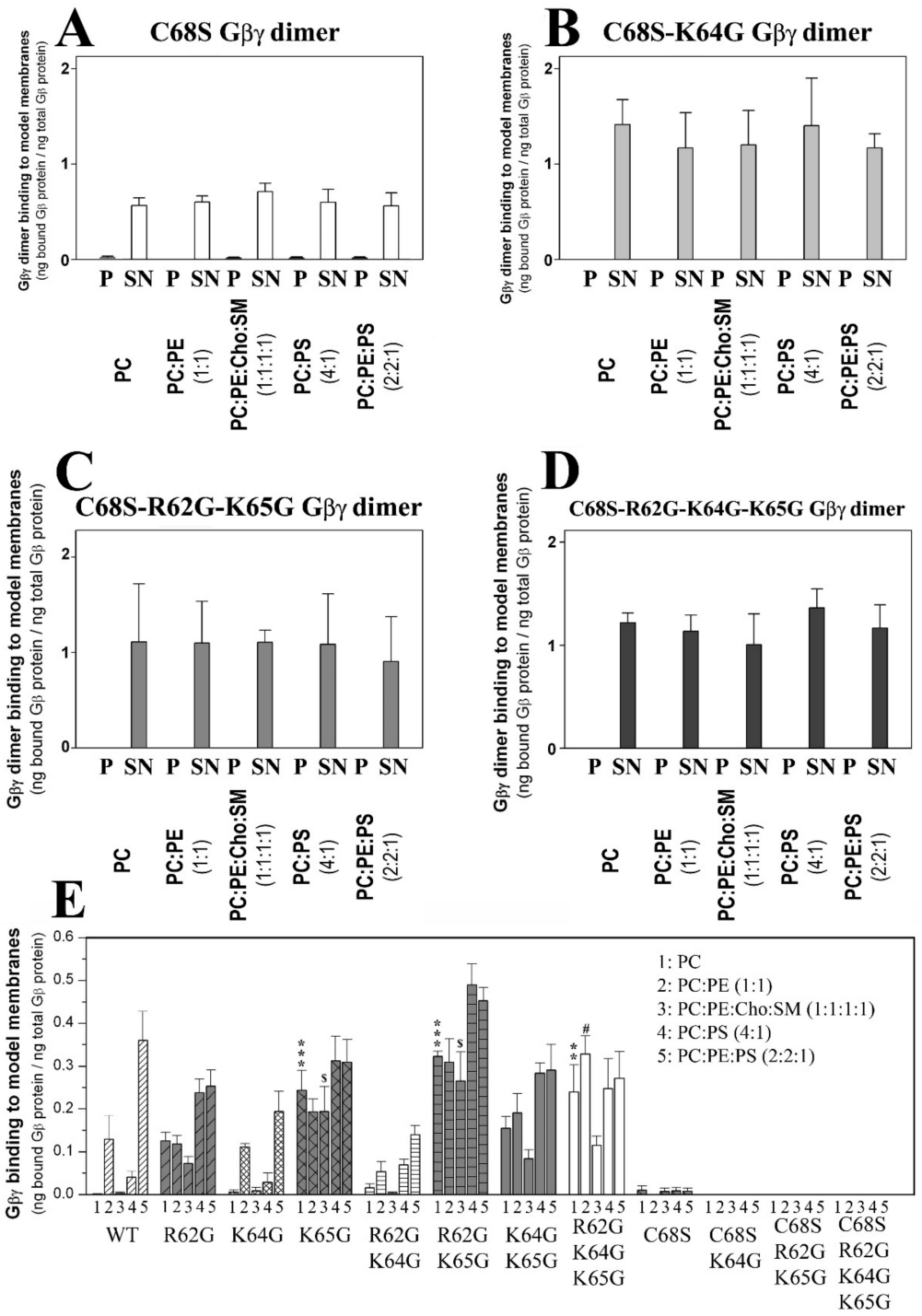

Figure 1. Effect of $G\gamma_2$ protein isoprenylation on $G\beta\gamma$–membrane interactions. (**A**), Binding of non-geranylgeranylated $G\beta_1\gamma_2$ to different model membranes that are representative of biological membrane microdomains. The Cys-68 (C68S) mutation is responsible for impeding geranylgeranylation. (**B**), Binding of the non-geranylgeranylated $G\beta_1\gamma_2$ dimer carrying gamma-subunit mutations of Lys-64 (K64G mutant) and Cys-68 to model membranes. (**C**), Binding of the non-geranylgeranylated $G\beta_1\gamma_2$ dimer carrying triple mutations of Arg-62 (R62G), Lys-65 (K65G) and Cys-68 to model membranes. (**D**), Binding of $G\beta_1\gamma_2$ carrying mutations of Arg-62, Lys-64, Lys-65 and Cys-68 to model membranes. In all cases, the binding of the dimer is calculated as the ng of bound $G\beta_1$ protein per ng of $G\beta_1$ protein in the medium. The molar ratios used are indicated between parentheses. Representative immunoblots of each binding experiment are shown in the Supplemental Material section. The data represent the mean ± S.E.M values. (**E**), $G\beta_1\gamma_2$ dimer binding to model membranes.

The graph shows the relative binding of the mutant and wild type (WT) dimers to different model membranes defined as ng of $G\beta_1$ bound relative to the total ng of $G\beta_1$ in the incubation medium. P, pellet (membrane fraction); SN, supernatant (soluble fraction). Symbols indicate significance (one, $p < 0.05$; two, $p < 0.01$; three, $p < 0.001$), where * corresponds to differences with respect to comparison with wild type G protein-PC interactions, # wild-type G protein-PC:PE interactions, and $ wild-type G protein-PC:PE:Cho:SM interactions.

3.2.2. Geranylgeranyl plus the Neighboring Basic Amino Acids Arg-62 and Lys-65 Drive $G\beta_1\gamma_2$ towards PE-Rich (Non-Lamellar Prone) L_d Membrane Microdomains

The interactions of geranylgeranylated $G\beta_1\gamma_2$ dimers with PE-rich model membranes (50% PE) were analyzed, with the K64G and R62G-K64G mutants showing a membrane binding profile similar to that of WT $G\beta_1\gamma_2$ (Figure 1E). Therefore, Lys-64 (K64G) did not play a relevant role in determining the preference of $G\beta_1\gamma_2$ for PE-rich microdomains (Figure 2A). In contrast, Arg-62 (R62G) and Lys-65 (R65G) were key amino acids in defining the preference of $G\beta_1\gamma_2$ for non-lamellar prone microdomains, although only Lys-65 was essential for this interaction (Figure 2). Hence, there was a relation between hydrophobicity in the $G\gamma_2$ C-terminal region, due to the introduction of serial mutations, and the decrease in the PC:PE-to-PC binding ratio (Figure 2B,C).

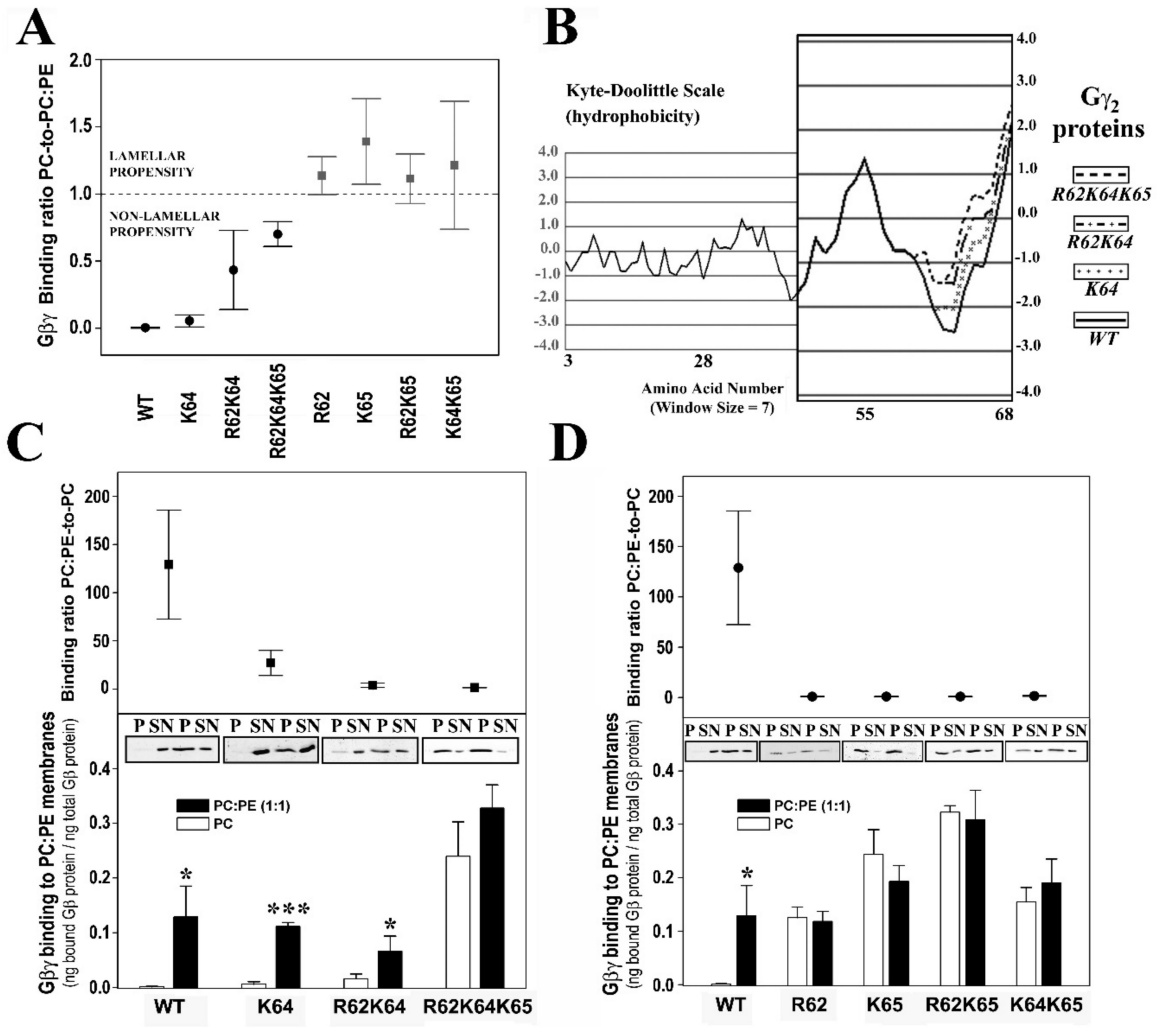

Figure 2. The influence of PE and $G\gamma_2$ structure on $G\beta\gamma$-membrane interactions. (**A**), Binding ratio PC-to-PC:PE corresponding to the different geranylgeranylated dimers are generated. The ratios

are calculated considering the fraction of $G\beta_1$ bound to PC relative to the corresponding fraction bound to PC:PE (1:1 molar ratio) in each independent experiment. (**B**), Profiles of hydrophobicity of four representative geranylgeranylated $G\beta_1\gamma_2$ dimers on the Kyte-Doolittle scale. The increasing hydrophobicity of these dimers is correlated with their increasing ratio of PC-to-PC:PE binding. (**C**), Binding preference of $G\beta_1\gamma_2$ dimers for lamellar-(PC) and non-lamellar-(PC:PE) prone membranes. In the upper panel, the PC:PE-to-PC binding ratio is depicted (bound Gβ1 protein relative to total $G\beta i_1$ protein). (**D**), Binding of $G\beta_1\gamma_2$ dimer mutants that have no preference for non-lamellar prone membrane structures to PC and PC:PE membranes with respect to the wild type dimer (WT). The upper and lower panels are equivalent to the panels shown in (**C**). Representative immunoblots of each binding experiment are also shown in (**C**,**D**). In all cases, the data represent the mean ± S.E.M: *** $p < 0.001$; * $p < 0.05$. All binding ratios in panel A, except for K64G, are significantly different from the control (WT) PC-to-PC:PE binding ratio ($p < 0.01$). Labels: WT, wild type; R62, R62G; K64, K64G; K65, K65G; *p*, pellet; SN, supernatant.

3.2.3. $G\gamma_2$ C-Terminal Basic Amino Acids Drive the Interaction of $G\beta_1\gamma_2$ with PS-Rich Membranes

The ratios of PC-to-PC:PS (20% PS) binding showed that Lys-65 was the most relevant amino acid for these membrane–Gβγ interactions, followed by Arg-62 and Lys-64 (Figure 3A). The absence of Lys-65 in the $G\gamma_2$ subunit of the heterodimer practically abolished the $G\beta_1\gamma_2$ binding preference to PS-rich membranes (Figure 3B). However, Arg-62 and Lys-64 contributed similarly to this phenomenon, as indicated by the binding profiles of the R62G-K65G and K64G-K65G double mutants (Figure 3B). The triple mutation of the basic amino acids to glycine abrogated the differential interaction between Gβγ and membranes with and without PS (Figure 3B).

3.2.4. Geranylgeranyl plus the Basic Arg-62, Lys-64 and Lys-65 Amino Acids Strongly Modulate the Interaction of $G\beta_1\gamma_2$ with PE- and PS-Rich Membranes

The $G\beta_1\gamma_2$ dimer exhibits a marked preference for membranes containing PE and PS, two major phospholipids with an asymmetrically higher distribution at the inner leaflet of the plasma membrane. The $G\gamma_2$ C-terminal region appears to be critical for the interaction of $G\beta_1\gamma_2$ heterodimer with membranes. Thus, single or multiple point mutations of R62G, K64G and K65G, in conjunction with the C68S mutation in the gamma subunit, reduced the affinity for PE- and PS-rich microdomains (Figure 3C). The remarkable differences in WT $G\beta_1\gamma_2$ binding to PC, PE and PS membranes contrasted with the relatively constant binding of the R62G-K64G-K65G $G\beta_1\gamma_2$ mutant to each of these different model membranes (Figure 3D). Hence, the $G\gamma_2$ C-terminal basic amino acids appear to be the key drivers of the preference of $G\beta_1\gamma_2$ for PE- and PS-rich microdomains (Figures 2C and 3D).

The presence of the two major phospholipids in the inner membrane monolayer produced a synergistic effect on Gβγ binding to membranes. This effect was dampened severely by the K64 mutation, and it was completely abolished by the R62G-K64G mutations (Figure 3E). Finally, heterodimers carrying the R62G, K64G-K65G, R62G-K65G and K65G mutations had a low affinity for PE-rich membranes, and they formed a group with very similar binding affinities to PC:PS and PC:PE:PS membranes (Figure 3C,F). These data clearly show co-operation between the geranylgeranyl moiety and its neighboring basic amino acids in terms of the interaction of the $G\beta_1\gamma_2$ heterodimer with model membrane microdomains containing PE and PS.

3.2.5. Arg-62 and Lys-65 Are Critical Residues in the Interaction between $G\beta_1\gamma_2$ and Ordered Lamellar Membranes

The Gβγ dimer prefers disordered (Ld) membrane microdomains. The isoprenoid lipid (ger) and Lys-65 are responsible for the reduced binding preference to ordered lamellar (raft-like) membranes, although the former is critical to favor G protein binding to membranes. Thus, the ability of $G\beta_1\gamma_2$ to interact with Lo membranes increased remarkably in the absence of Lys-65 (K65G: Figure 3G). Arg-62 (R62G) mutation also reduced the

heterodimer's binding preference to lamellar membranes and its preference for Ld-like microdomains. Finally, both Lys-64 and Lys-65 (i.e., the K64G-K65G and R62G-K64G-K65G mutants) also drove the preference of the dimer for PC-rich membranes with respect to raft-like membranes (Figure 3G).

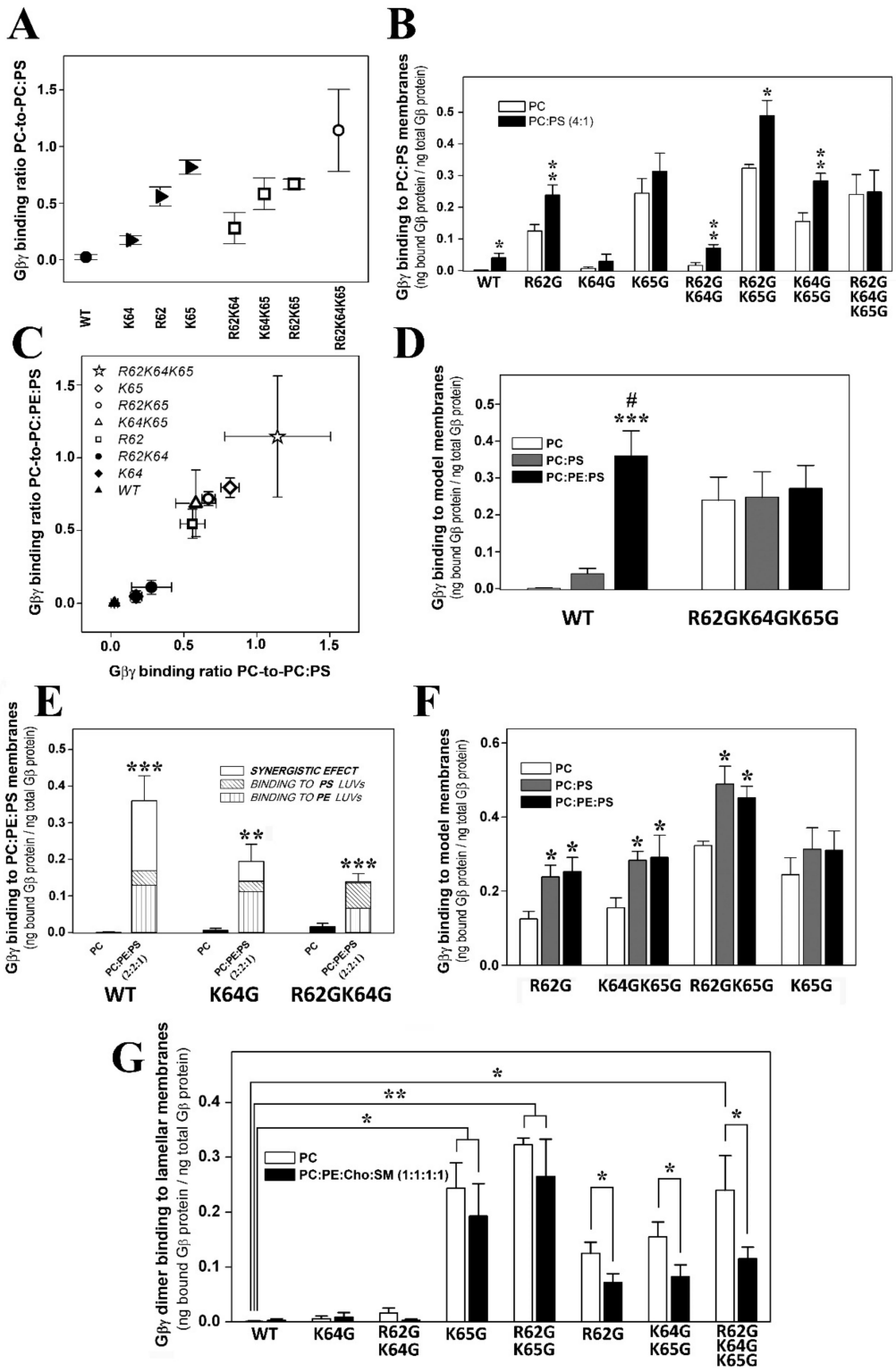

Figure 3. Roles of PS and $G\gamma_2$ structures on $G\beta\gamma$–membrane interactions. (**A**), PC-to-PC:PS binding ratios corresponding to the different geranylgeranylated dimers. The wild-type dimer is depicted as

a solid circle and the triple mutant as an open circle, whereas single mutants are depicted as solid triangles and the double mutants as open squares. (**B**), Binding of geranylgeranylated $G\beta_1\gamma_2$ dimers to PC and PC:PS (4:1, mol:mol) membranes. The binding of the dimer is calculated as the bound $G\beta i_1$ protein relative to the total $G\beta_1$ protein (n = 3–8). Asterisks indicate significant differences (* $p < 0.05$; ** $p < 0.01$) with respect to PC membranes. (**C**), PC-to-PC:PE:PS binding ratio vs. the PC-to-PC:PS binding ratio. In this graph, the solid symbols represent the dimers with the greatest preference for PC:PE membranes, while the open symbols correspond to dimers with low or no preferential binding. (**D**), Binding of the WT and R62GK64GK65G mutant $G\beta_1\gamma_2$ dimers to PC, PC:PS and PC:PE:PS (2:2:1, mol:mol:mol) membranes. The bars represent the mean values of the dimer bound to these three model membranes (bound $G\beta_1$ protein relative to total $G\beta_1$ protein, n = 4). Significant differences with respect to PC (*** $p < 0.001$) and to PC:PS (# $p < 0.05$) membranes are found. (**E**), Binding of WT, K64G and R62GK64G $G\beta_1\gamma_2$ dimers to PC and PC:PE:PS membranes. Binding is calculated as in (**B**,**D**) (n = 3–4), and the bars corresponding to the total binding to PC:PE:PS membranes are divided into three parts: that representing the binding to PC:PE; that representing the binding to PC:PS; and a third part reflecting a possible synergistic effect. Significant differences (** $p < 0.01$; *** $p < 0.001$) with respect to PC membranes are found. (**F**), Binding of the R62G, K65G, K64GK65G and R62GK65G $G\beta_1\gamma_2$ dimers to PC, PC:PS and PC:PE:PS membranes. * $p < 0.05$ with respect to PC. (**G**), Binding of the WT, K64G, R62GK64G, K65G, R62GK65G, R62G, K64GK65G and R62GK64GK65G $G\beta_1\gamma_2$ dimers to PC (open bars) and PC:PE:Cho:SM (solid bars) membranes. The binding is calculated as in (**B**,**D**,**E**) (n = 3–8). The data represent the mean ± S.E.M.: *** $p < 0.001$; ** $p < 0.01$; * $p < 0.05$. '#' indicates significant differences in the binding of $G\beta_1\gamma_2$ to PC:PE:PS with respect to its binding to PC:PS. All binding ratios in panels (**A**,**C**) are significantly different from the corresponding control (WT) PC-to-PC:PS and PC-to-PC:PE:PS binding ratios ($p < 0.05$).

3.2.6. Geranylgeranylation Drives the Localization of $G\gamma_2$ and $G\beta_1\gamma_2$ to Biological Membranes

In Sf9 cells, the Lys-64 mutation did not influence the binding of $G\gamma_2$ to membranes, while the absence of geranylgeranylation led to the localization of $G\gamma_2$ to the cytosol when overexpressed alone (Figure S4). Following its overexpression, WT $G\beta_1$ accumulated in the membrane fraction (Figure S4), which could be explained by the possible aggregation of $G\beta_1$ monomers due to the excess of this subunit relative to endogenous Gα and Gγ proteins. However, when both proteins were co-expressed, WT $G\beta_1$ with $G\gamma_2$ C68S-K64G mutant further shifted the binding profile of WT $G\beta_1$ 1 as well as that of $G\gamma_2$, which were both even more prominent in the cytosol (Figure S5).

3.3. Effects of the $G\gamma_2$ C-Terminal and $G\alpha i_1$ N-Terminal Regions and Membrane Lipid Organization on $G\alpha i_1\beta_1\gamma_2$-Membrane Interactions

In general, the binding of $G\alpha i_1\beta_1\gamma_2$ to lipid bilayers with different composition was closer to that of the dimer and diverted from the membrane binding behavior of the monomer, although the acyl moieties on $G\alpha i_1$ also induced modest modulation of heterotrimer–lipid interactions.

3.3.1. Geranylgeranyl and Myristoyl Moieties Are Required for $G\alpha i_1\beta_1\gamma_2$ Targeting to PE-Rich Non-Lamellar Prone Microdomains

There was a clear preference of geranylgeranylated and myristoylated $G\alpha i_1\beta_1\gamma_2$ heterotrimers to bind to PE-rich (PC:PE, 1:1, mol:mol) membranes with a high non-lamellar propensity (Figure 4A). Thus, myristoylated and isoprenylated and non-palmitoylated (a naturally occurring trimer form) bound significantly more to PE-rich membranes than to PC membranes (Figure 4B). The absence of the myristoyl moiety in these complexes abolished their preference for non-lamellar prone membranes (Figure 4A,B), as evident when the heterotrimers were detected with different antibodies against the $G\alpha i_1$ or $G\beta_1$ subunits (Figure 4B). However, mutations in the $G\gamma_2$ polybasic domain did not significantly affect the interaction of the different trimers with PC:PE membranes (Figure 4).

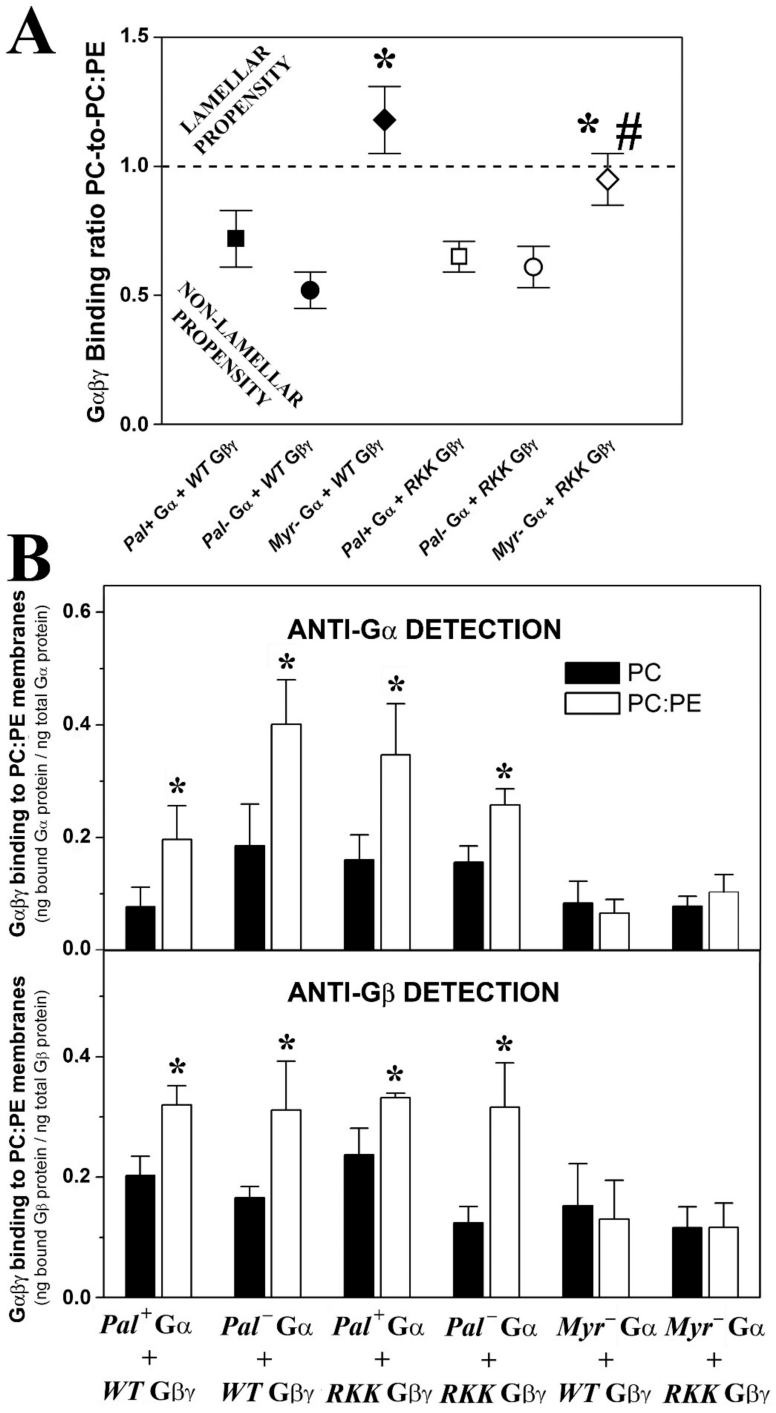

Figure 4. Effect of PE and Gαi$_1$ and Gγ$_2$ structures on Gαβγ–membrane interactions. (**A**), Binding ratio PC-to-PC:PE corresponding to the different Gαi$_1$β$_1$γ$_2$ heterotrimers generated and purified. The ratios are calculated considering the fractions of Gαi$_1$ and Gβ$_1$ bound to PC relative to their corresponding fractions of binding to PC:PE (1:1, mol:mol) in each independent experiment. The data represent the mean ± S.E.M. values: * $p < 0.05$ with respect to Pal+ Gαi$_1$/WT Gβ$_1$γ$_2$; # $p < 0.05$ with respect to Myr- Gαi$_1$/WT Gβ$_1$γ$_2$. (**B**), Binding of Gαi$_1$β$_1$γ$_2$ heterotrimers to PC and PC:PE membranes. Bars show the mean binding of the heterotrimers to PC and PC:PE membranes calculated as the bound Gαi$_1$ protein relative to total Gαi$_1$ protein (upper panel) or bound Gβ$_1$ protein relative to total Gβ$_1$ protein (lower panel). It has to be noticed that palmitoylation is reversible, so that Pal- is not a mutant but a natural status of the monomeric and trimeric G protein forms. RKK: R62G-K64G-K65G. The data represent the mean ± S.E.M.: * $p < 0.05$.

3.3.2. $G\alpha i_1$ Myristoylation and Palmitoylation and the $G\gamma_2$ C-Terminal Polybasic Domain Regulate $G\alpha i_1\beta_1\gamma_2$-PS Interactions

Geranylgeranylated and myristoylated (and non-palmitoylated) $G\alpha i_1\beta_1\gamma_2$ heterotrimers bound significantly better to PC:PS membranes (PC: PS, 3:2, mol:mol) than to PC membranes (Figure 5). Triple mutation of the $G\gamma_2$ C-terminal basic amino acids in combination with palmitoylation of the $G\alpha i_1$ subunit dramatically reduced the behavior of the geranylgeranylated and myristoylated $G\alpha i_1\beta_1\gamma_2$ heterotrimer, particularly in terms of its interaction with PS-rich membranes (PC:PS, 3:2, mol:mol). In addition, the lack of the myristoyl moiety abolished the preference of $G\alpha i_1\beta_1\gamma_2$ for PS-rich membranes. Again, similar results were obtained when the binding of heterotrimeric G proteins to model membranes was measured with both the anti-$G\alpha i_1$ or anti-$G\beta_1$ antibodies, supporting the appropriateness of this technique (Figure 5 and Figure S6D).

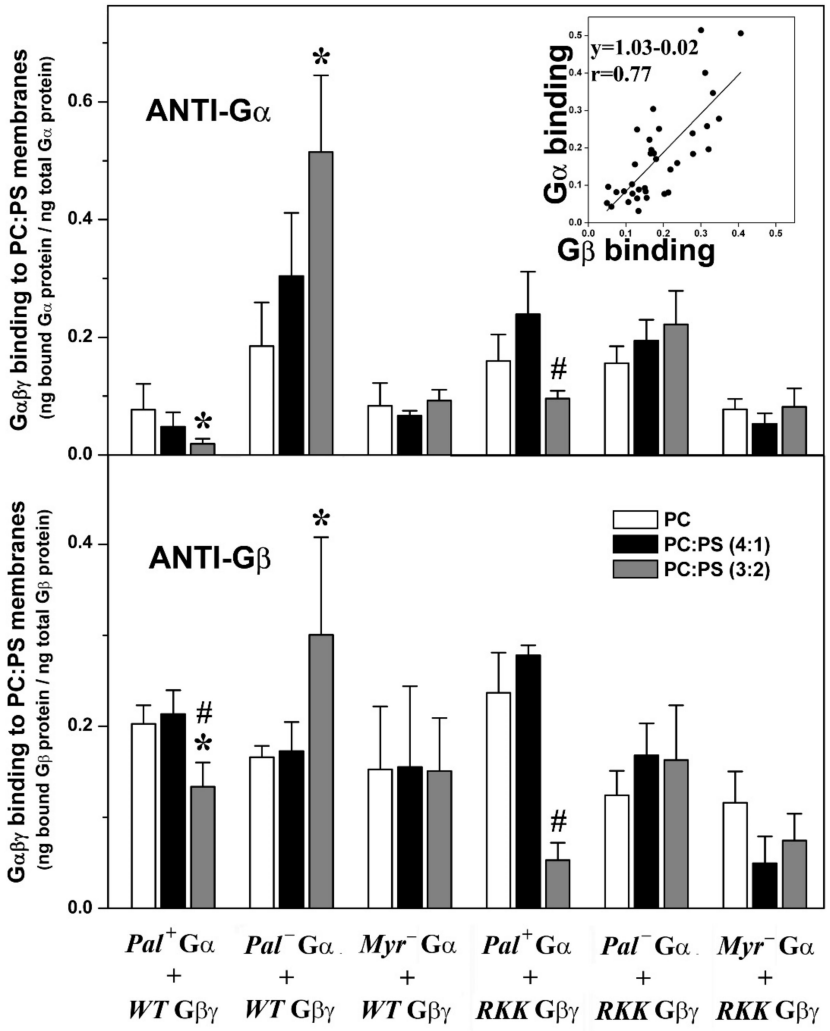

Figure 5. Effects of PS and the $G\alpha i_1$ and $G\gamma_2$ structures on $G\alpha\beta\gamma$–membrane interactions. In the upper panel, the bars show mean ± S.E.M. values of $G\alpha i_1\beta_1\gamma_2$ heterotrimer binding to PC and PC:PS (4:1 and 3:2, mol:mol) membranes, which is calculated as the bound $G\alpha i_1$ protein relative to total $G\alpha i_1$ protein. In the lower panel, binding is calculated as the bound $G\beta_1$ protein relative to total $G\beta i_1$ protein. The inset shows the correlation between the binding for the G proteins investigated in the present study as measured with anti-$G\alpha i_1$ and -$G\beta_1$ antibodies using the same samples. The patterns of the bars in the lower panel are equivalent to those in the upper panel. RKK: R62G-K64G-K65G. Data correspond to 2–6 independent experiments, and "*" ($p < 0.05$) indicates significant differences with respect to PC membranes, whereas "#" ($p < 0.05$) indicates significant differences in the binding of $G\alpha i_1\beta_1\gamma_2$ to PC:PS (3:2, mol:mol) with respect to its binding to PC:PS (4:1, mol:mol).

3.3.3. Myristoylated and Non-Palmitoylated $G\alpha i_1\beta_1\gamma_2$ Complexes Have a High Affinity for PE- and PS-Rich Membrane Microdomains

The binding of myristoylated, geranylgeranylated and non-palmitoylated $G\alpha i_1\beta_1\gamma_2$ heterotrimers to PC, PC:PE (PC:PE, 1:1, mol:mol) and PC:PE:PS (PC:PE:PS, 2:2:1, molar ratio) membranes were qualitatively similar to that observed for $G\beta_1\gamma_2$ (Figure 6A). This important result further explained and demonstrated the decisive role of $G\beta\gamma$ dimer in the localization of $G\alpha i\beta\gamma$ heterotrimers to non-lamellar prone membrane microdomains [24]. None of the other mutated heterotrimers studied here displayed this behavior in regard to their interaction with PE- and PS-rich membranes (Figure 6B). Thus, the myristoylated, geranylgeranylated and non-palmitoylated heterotrimers preferentially bound to PC:PE membranes than to PC, and the presence of 20 mol% PS further enhanced the interaction of these complexes with membranes (Figure 6C,D). The triple $G\gamma_2$ mutant, the myristoylated complex containing the R62G-K64G-K65G mutations, interacted less with PC:PE:PS membranes (Figure 6E,F). In fact, this interaction was very similar to the interaction with PC, which suggests a decisive role of the three C-terminal basic amino acids of $G\gamma_2$ in the localization of $G\alpha i_1\beta_1\gamma_2$ to membrane microdomains with a high non-lamellar propensity and a negative charge, such as those rich in PE and PS that are the most abundant phospholipids in the inner layer of the plasma membrane [32].

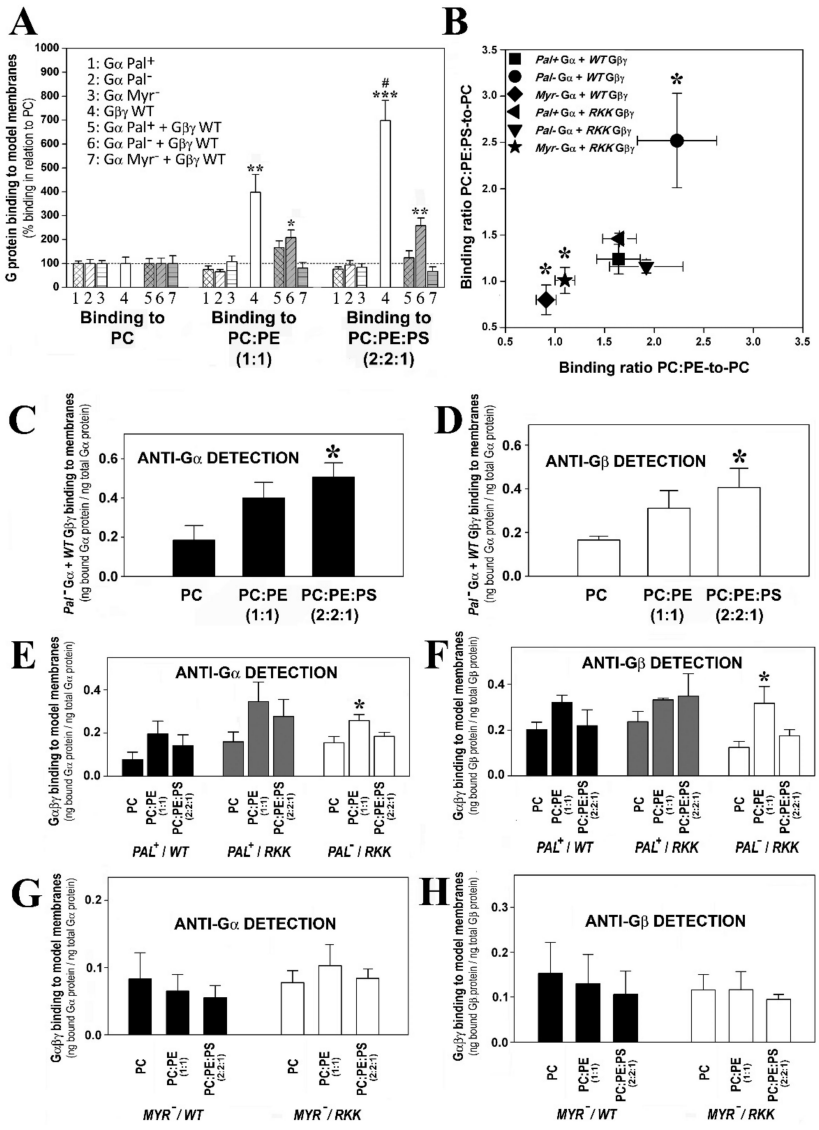

Figure 6. Effect of the major P-face membrane lipids, PS and PE and $G\alpha i_1/G\gamma_2$ structure on the $G\alpha\beta\gamma$-membrane interactions. (**A**), Graph of the global G protein–membrane interactions. Binding of

the G protein monomers, Pal+ $G\alpha i_1$, Pal− Myr$^-$ (G2A mutant) $G\alpha i_1$ the WT $G\beta_1\gamma_2$ dimer, and the heterotrimers, WT $G\beta_1\gamma_2$-Pal+ $G\alpha i_1$, WT $G\beta_1\gamma_2$-Pal$^-$ (C3S mutant) $G\alpha i_1$ and WT $G\beta_1\gamma_2$-Myr$^-$ $G\alpha i_1$, to PC, PC:PE (1:1, mol:mol) and PC:PE:PS (2:2:1, mol:mol). The bars represent the mean binding of G proteins to these three model membranes calculated as % binding relative to that to PC, considering the fraction of binding to PC as 100%. The asterisks indicate the significant differences in the binding of G proteins to membranes with respect to its binding to PC (*** $p < 0.001$; ** $p < 0.01$; * $p < 0.05$), while '#' indicates significant differences ($p < 0.05$) in the binding of G proteins to PC:PE:PS with respect to its binding to PC:PE. (**B**), Binding ratio PC:PE:PS-to-PC vs. binding ratio PC:PE-to-PC. Each ratio is calculated considering the fraction of binding to PE membranes relative to the fraction of binding to PC in each independent experiment, and significant differences with respect to Pal+ $G\alpha i_1$/WT $G\beta_1\gamma_2$ are indicated (* $p < 0.01$). RKK: R62G-K64G-K65G. (**C**,**D**), Binding of WT $G\beta_1\gamma_2$-Pal$^-$ $G\alpha i_1$ to PC, PC:PE and PC:PE:PS membranes. (**E**,**F**), Binding of WT $G\beta_1\gamma_2$-Pal+ $G\alpha i_1$ (black bars), RKK $G\beta_1\gamma_2$-Pal+ $G\alpha i_1$ (grey bars) and RKK $G\beta_1\gamma_2$-Pal$^-$ $G\alpha i_1$ (white bars) to PC, PC:PE and PC:PE:PS membranes. (**G**,**H**), Binding of WT $G\beta_1\gamma_2$-Myr$^-$ $G\alpha i_1$ (black bars) and RKK (R62G, K64G, K65G mutant) $G\beta_1\gamma_2$-Myr− $G\alpha i_1$ (white bars) to PC, PC:PE and PC:PE:PS membranes. In (**C**,**E**,**G**), the bars represent the mean value of the α subunit binding to membranes (bound $G\alpha i_1$ protein relative to total $G\alpha i_1$ protein). In (**D**,**F**,**H**), the bars represent the mean value of the β subunit binding to membranes (bound $G\beta_1$ protein relative to total $G\beta_1$ protein). The data represent the mean ± S.E.M. values: * $p < 0.05$.

The two studied palmitoylated $G\alpha i_1\beta_1\gamma_2$ heterotrimers had PC:PE:PS-to-PC and PC:PE-to-PC binding ratios that very close to the ratios of R62G-K64G-K65G $G\beta\gamma$-Pal− $G\alpha i_1$ (Figure 6B), and their corresponding binding profiles did not differ significantly, further supporting that both structural features (i.e., lipid moiety and $G\gamma_2$ polybasic domain) are relevant in the microdomain segregation of G protein trimers (Figure 6E,F).

Finally, the two studied non-myristoylated and geranylgeranylated heterotrimers did not show significant lipid binding preferences, with binding ratio values close to 1 (Figure 6B). Binding of these complexes to PC, PC:PE and PC:PE:PS membranes were very similar in all the cases, demonstrating that the mutants lost the ability of segregating to different membrane microdomains (Figure 6G,H).

3.3.4. $G\alpha i_1$ Myristic Acid and C-Terminal $G\gamma_2$ Basic Amino Acids Prevent $G\alpha i_1\beta_1\gamma_2$ Targeting to Raft-Like Membrane Domains

The non-palmitoylated WT $G\alpha\beta\gamma$ protein displayed similar affinity for PC membranes and raft-like (PC:PE:SM:Cho) membranes, whereas the heterotrimer lacking myristic acid on the alpha subunit (WT $G\beta_1\gamma_2$-Myr$^-$ $G\alpha i_1$: G2A alpha subunit mutant) showed higher binding affinity for lamellar prone (PC) membranes. Conversely, the R62G-K64G-K65G $G\beta_1\gamma_2$-Myr$^-$ $G\alpha i_1$ complex displayed a clear preference for raft-like membranes (Figure 7A). In fact, this mutant showed higher binding affinity to raft-like membranes (PC:PE:Cho:SM, 1:1:1:1, mol ratio) than to PC membranes, a behavior that contrasts with that of wild type heterotrimers that apparently prefer to bind to non-raft PC membranes (Figure 7B).

3.4. The $G\alpha i_1$ Monomer and the Corresponding Heterotrimer Differ Remarkably in Their Binding to Membranes

The Pal+ $G\alpha i_1$ monomer bound more intensely to PC, PC:PS (3:2, mol:mol) and PC:PE:Cho:SM (1:1:1:1, mol:mol) membranes than the WT $G\beta_1\gamma_2$ -Pal+ $G\alpha i_1$ heterotrimer (Figure 8, upper panel). In contrast, the binding of the WT $G\beta_1\gamma_2$ -Pal$^-$ $G\alpha i_1$ (C3S $G\alpha i_1$ mutant) heterotrimer to non-lamellar prone membranes of PC:PE (1:1, mol:mol) and PC:PE:PS (2:2:1, mol:mol) was significantly higher than that of the Pal$^-$ $G\alpha i_1$ monomer (Figure 8, middle panel). In all cases, significantly more of the heterotrimeric Myr$^-$ (G2A mutant) $G\alpha i_1$ protein bound to model membranes than the corresponding monomer (Figure 8, lower panel). Heterotrimeric Myr$^-$ $G\alpha i_1$ also bound to biological membranes significantly more than the corresponding monomeric form. The Myr$^-$ $G\alpha i_1$ protein bound most intensely to

biological (Sf9 cell) membranes influenced by $G\beta_1\gamma_2$ (37%), followed by Pal^- $G\alpha i_1$ (23%) and finally by WT $G\alpha i_1$ (18%) (Figure S7).

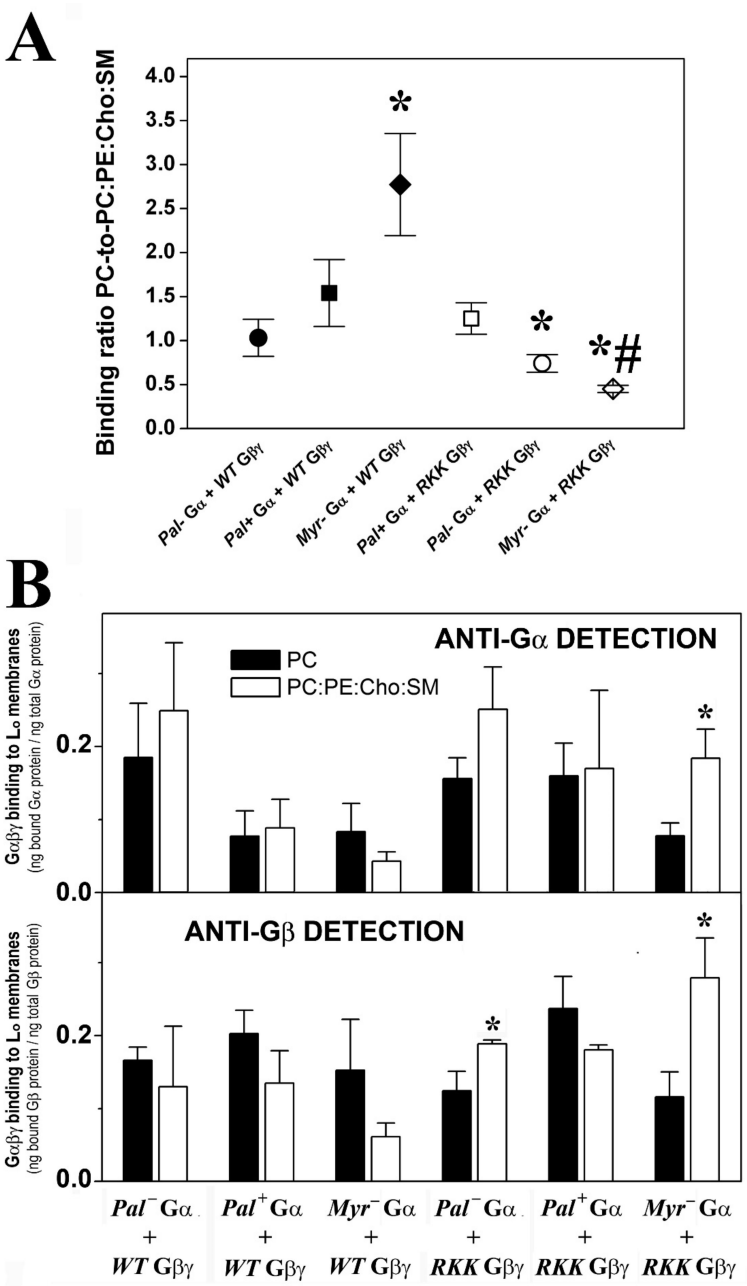

Figure 7. Effect of membrane lipid order and $G\alpha i_1/\gamma_2$ structure on $G\alpha\beta\gamma$–membrane interactions. (**A**), PC-to-PC:PE:Cho:SM binding ratio of the different $G\alpha i_1\beta_1\gamma_2$ heterotrimer constructs. The ratios are calculated considering the respective $G\alpha i_1$ and $G\beta_1$ fractions bound to PC relative to their corresponding fractions bound to PC:PE:Cho:SM (1:1:1:1, mol:mol) in each independent experiment. The data represent the mean ± S.E.M. values: * $p < 0.05$ with respect to PC membranes; # $p < 0.05$. (**B**), Binding of $G\alpha i_1\beta_1\gamma_2$ heterotrimers to PC and PC:PE:Cho:SM membranes. The bars in the upper panel show the mean binding of the heterotrimers to PC and PC:PE:Cho:SM membranes, calculated as the bound $G\alpha i_1$ subunit relative to the total $G\alpha i_1$ subunit. In the lower panel, the binding is calculated as the bound $G\beta_1$ subunit relative to the total $G\beta_1$ subunit. The colors of the bars in the lower panel are equivalent to those in the upper panel and in both panels representative immunoblots of each binding experiment are shown. The data represent the mean ± S.E.M.: * $p < 0.05$ with respect to PC membranes.

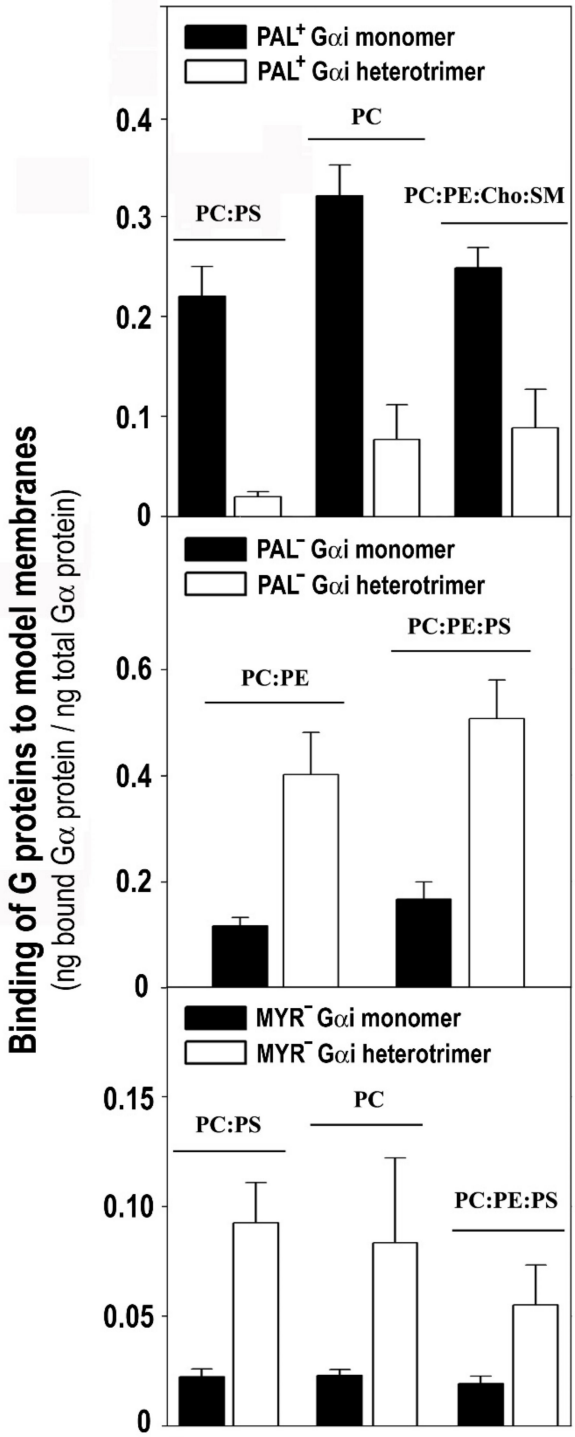

Figure 8. Comparative binding of $G\alpha i_1$ monomer and $G\alpha i_1\beta_1\gamma_2$ trimer to membranes with different lipid composition. This graph shows the most relevant differences in the membrane-binding properties of the $G\alpha i_1$ protein in its monomeric and trimeric forms. Upper panel, Comparative binding of monomeric Pal^+ $G\alpha i_1$ and trimeric WT $G\beta_1\gamma_2$-Pal^+ $G\alpha i_1$ complex to PC:PS (3:2, mol:mol), PC and PC:PE:Cho:SM (1:1:1:1, mol:mol). The greatest differences in binding between these Pal^+ $G\alpha i_1$ proteins were observed in these cases. Middle panel, Comparative binding of monomeric Pal^- $G\alpha i_1$ and trimeric *WT* $G\beta_1\gamma_2$-*Pal*$^-$ $G\alpha i_1$ heterotrimer to PC:PE (1:1, mol:mol) and PC:PE:PS (2:2:1, mol:mol). Lower panel, Comparative binding of monomeric Myr^- (G2A mutant) $G\alpha i_1$ and trimeric WT $G\beta_1\gamma_2$-Myr^- $G\alpha i_1$ complex to PC:PS (3:2, mol:mol), PC and PC:PE:PS (2:2:1, mol:mol). All bars are mean ± S.E.M. values and in all cases $p < 0.05$ for each monomer-trimer pair.

3.5. The Myristoyl and Geranylgeranyl Moieties Plus the Gγ$_2$ C-Terminal Polybasic Domain Are Key Determinants of the Interaction of Gαi$_1$β$_1$γ$_2$ with Biological Membranes

Myristic acid is essential in the interaction of G protein monomers or trimers with biological membranes. Thus, a mutation on the Gαi$_1$ N-terminal glycine induced a significant loss of protein binding to Sf9 membranes relative to Pal$^-$ (C3S) Gαi$_1$ and WT Gαi$_1$ (Figure S8). Nevertheless, the increase in the binding of the Myr$^-$ (G2A) Gαi$_1$ heterotrimeric form relative to the monomer was noteworthy, as indicated previously.

Geranylgeranylation had a more significant impact than myristoylation on the ability of the three subunits to interact with biological membranes. Thus, the ger$^-$ K64G-C68S double Gγ$_2$ mutant significantly modified the binding of Gαi$_1$, Gβ$_1$ and Gγ$_2$ to cell membranes, unlike the K65G-C68S mutant (Figure S9). These results clearly demonstrate the importance of the C-terminal Gγ$_2$ basic amino acids in the interactions of Gαi$_1$β$_1$γ$_2$ with Sf9 cell membranes.

4. Discussion

Here, it was showed that the N-terminal region of Gαi$_1$ (Myr- and Pal- mutants: G2A and C3S mutations) influence its interaction with membranes and that of the trimeric Gαi$_1$β$_1$γ$_2$ protein. However, the membrane binding and microdomain sorting of the latter receive a greater influence from the C-terminal region of the Gγ$_2$ subunit (C68S, R62G, K64G and K65G mutations), which has a membrane interaction pattern similar to that of the Gβ$_1$γ$_2$ dimer with slight modifications. In this context, the activity of G proteins is modulated significantly by protein–lipid interactions [24,35,36], and hence, we investigated the role of G protein structure and membrane composition on the membrane preference of monomeric, dimeric and trimeric forms of these proteins. To this end, model lipid membranes with a defined lipid composition were generated to test the binding of highly purified G proteins with specific mutations in the α and γ subunits. These new findings showing the role of lipid modifications and polybasic domain in G protein–membrane interactions, which support the previous suggestion about structure–function relationship on G protein interactions with lipids. These interactions, which remain largely unknown, are critical for cell signal propagation, and their alterations are involved in pathological processes and therapeutic approaches [47,48].

In this context, Gβ$_1$γ$_2$ dimer binding to negatively charged and non-lamellar prone lipid membranes apparently relies on the geranylgeranyl moiety and a neighboring Gγ$_2$ polybasic domain that includes residues Arg-62, Lys-64 and Lys-65. In a previous study, we noted that the C-terminal region of the Gγ$_2$ subunit regulated its subcellular localization [6]. Here, we found that geranylgeranyl and Lys-65 were minimal requirements to drive Gβ$_1$γ$_2$ to non-lamellar prone (PE-rich) microdomains. The binding of the Gβ$_1$γ$_2$ dimer to PE-rich domains was also regulated by Arg-62, and consequently, the R62G-K65G mutant was unable to bind preferentially to PE-rich non-lamellar prone membrane domains (Figure 9E). Conversely, the mutation of Lys-64 (K64G) did not dramatically affect the membrane binding of Gβ$_1$γ$_2$. In addition, all these basic amino acids participated in the direct binding of Gβ$_1$γ$_2$ to PS. Thus, the absence of the polybasic domain of Gγ$_2$ completely abolished Gβ$_1$γ$_2$-binding to PS and its remarkable preference for PE- and PS-rich microdomains, the main phospholipids at the inner monolayer of the plasma membrane [32], and this indicates electrostatic protein–lipid interactions, as suggested by previous studies using confocal microscopy in live cells [6]. This study demonstrates that all the Gγ$_2$ C-terminal modifications (isoprenylation, methylation and polybasic domain) have a differential role in G protein–lipid interactions.

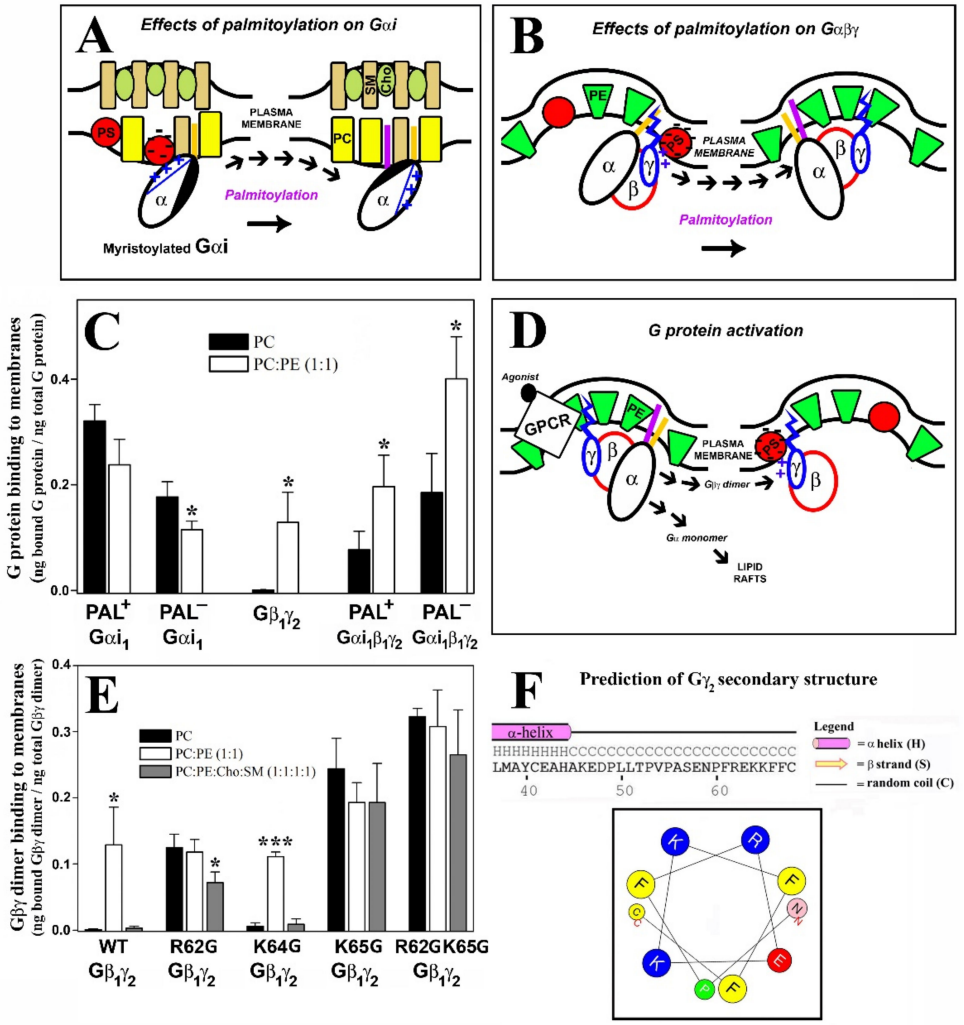

Figure 9. Key molecular determinants of Gαi1β1γ2-membrane interactions and models to explain the G protein-lipid membrane interactions. (**A**), Model to explain the interaction between Gαi1 and membrane lipids. A reorientation of the N-terminal α helix of Gαi1 by reversible palmitoylation of the protein drives its redistribution in the plasma membrane, moving it from PS-rich toward PS-poor raft-like microdomains. (**B**), Model to explain the Gαi1β1γ2-membrane interactions depending on the palmitoylation status of the protein G complex. Localization of palmitoylated Gαi1β1γ2 to PS-poor and PE-rich microdomains differs from the distribution of de-palmitoylated Gαi1β1γ2 in PS- and PE-rich microdomains. (**C**), Graph showing the nonlamellar preference and the role of reversible palmitoylation in the basic mechanisms of Gαi, Gβγ and Gαiβγ interactions with membrane lipids. Bars represent the binding of Pal+ Gαi1, Pal− (C3S mutant) Gαi1, WT Gβ1γ2, WT Gβ1γ2-Pal+ and WT Gβ1γ2-Pal− Gαi1 to PC and PC:PE (1:1, mol:mol) membranes. (**D**), Model of the activation of heterotrimeric G proteins that explains the interaction of Gαi1β1γ2 with membrane lipids in the presence of GPCR and the migration of the Gβ1γ2 dimer after its separation from Gα. (**E**), Graph showing representative results of the WT and mutated Gβ1γ2 dimer's interactions with model membranes. Bars represent the binding of WT Gβ1γ2, single mutants and the R6G2K65G Gβ1γ2 mutant to PC, PC:PE (1:1, mol:mol) and PC:PE:Cho:SM (1:1:1:1, mol:mol) membranes to show the role of the γ2-subunit C terminal amino acids in the G protein dimer interactions with lamellar- and nonlamellar-prone membrane microdomains. (**F**), Secondary structure predictions of the C-terminal region of Gγ2 using the Psi-Pred and HELIQUEST tools. A bi-dimensional projection of the hypothetical C-terminal α helix of Gγ2 is depicted considering the last 10 amino acids of the protein (N and C represent the N- and C-terminal amino acids of this region, which coincidentally coincide with the amino acids asparagine, N, and cysteine, C, respectively). In (**C**,**E**), the data represent the mean ± S.E.M.: *** $p < 0.001$; * $p < 0.05$.

Our results suggest that there is a specific structured interaction between the three basic amino acids studied and membrane lipids, in contrast with the data published that suggests the C-terminal $G\gamma_2$ region is disordered in the absence of membranes [49,50]. These previous studies give thorough and precise data about the overall α, β and γ subunit interactions, but the facts that the γ_2 subunit had a C68S mutation that prevents its prenylations and no lipids were present in the medium could influence the structure elucidation of this small amino acid region. Current signaling models based on X-ray diffraction studies (Figure 10, [49]) consider the critical role of G protein lipids but not the exposure of charged amino acids to the membrane surface [51]. A structural prediction of the $G\gamma_2$ C-terminal region using PSIPRED confirmed previous X-ray diffraction results, since this simulation showed a disordered structure without regular spatial organization ('random coil'). However, our results suggest the appearance of a transient structured conformational state for the C-terminal region of $G\gamma_2$ that interacts with the membrane lipid bilayer. In this model, confirmed by a bi-dimensional computer-assisted projection (Figure 9F), Arg-62 and Lys-65 would be very close to the polar membrane surface and near the geranylgeranyl moiety, whereas Lys-64 would be located at a distance in the turn of a small α-helix. This structure justifies the differential role of these basic amino acids in the interaction with negatively charged, PS-rich membranes.

Concerning $G\alpha i_1\beta_1\gamma_2$ heterotrimers, the different acylated variants shared membrane lipid preferences with the $G\beta_1\gamma_2$ dimer, which differ from those of the $G\alpha i_1$ monomer. These results further confirm and extend the pivotal role of the Gβγ dimer in Gαβγ–membrane interactions [24,35,36]. Thus, the preferential targeting of all the studied myristoylated and geranylgeranylated $G\alpha i_1\beta_1\gamma_2$ complexes to PE-rich microdomains were observed. Therefore, myristoyl and geranylgeranyl moieties (irreversibly and permanently present in this G protein trimer) are key determinants of the binding of $G\alpha i_1\beta_1\gamma_2$ to these non-lamellar prone membrane microdomains with a negative curvature strain, quite distinct from the more ordered membrane microdomains. Both these lipid modifications may be required to prevent Gαβγ localization into ordered lamellar membranes, such as lipid rafts. The high lipid packing density (i.e., high lateral surface pressure) in these membrane domains reduces the number of available gaps or "membrane defects" for the insertion of bulky lipids (e.g., geranylgeranyl). Conversely, the loose surface packing and membrane defects in non-lamellar prone membranes would facilitate the insertion of the myristoyl and geranylgeranyl moieties and even that of palmitic acid.

Previously, we demonstrated that Gβγ drives Gα from highly ordered lipid microdomains (L_o) to disordered microdomains (L_d) with a high curvature strain [24,35,36]. Here, we showed that palmitoylated $G\alpha i_1\beta_1\gamma_2$ and de-palmitoylated $G\alpha i_1\beta_1\gamma_2$ prefer non-lamellar prone model membranes, although the latter showed a higher binding capacity to membranes (Figure 9C). However, they differed significantly in their interaction with phosphatidylserine. Thus, while the myristoylated heterotrimer (WT $G\beta_1\gamma_2$-Pal^- $G\alpha i_1$: C3S $G\alpha i_1$ mutant) bound to PS-rich membranes (PC:PS and PC:PE:PS), palmitoylation disturbed the interaction of the heterotrimer with PS and even provoked electrostatic repulsion (Figure 5). Thus, the natural presence or absence of reversibly bound palmitoyl moiety regulated the interaction of $G\alpha i_1\beta_1\gamma_2$ with membranes, as described for $G\alpha i_1$ [35]. Interestingly, the palmitoylated heterotrimer that includes a $G\gamma_2$ subunit with mutations of Arg-62 (R62G), Lys-64 (K64G) and Lys-65 (K65G) had a similar binding profile to PS. This can be explained if the C-terminal basic amino acids of $G\gamma_2$ do not interact with membranes in palmitoylated $G\alpha i_1\beta_1\gamma_2$. These results support the structure-based interaction of the C-terminal region of the gamma subunit with membranes and the role of the palmitoyl moiety in the regulation of protein structure and G protein–membrane interactions. Nevertheless, the Gβγ dimer again seems to be crucial in this interaction, more precisely, the $G\beta_1$ protein (Figures 9B,D and 10A).

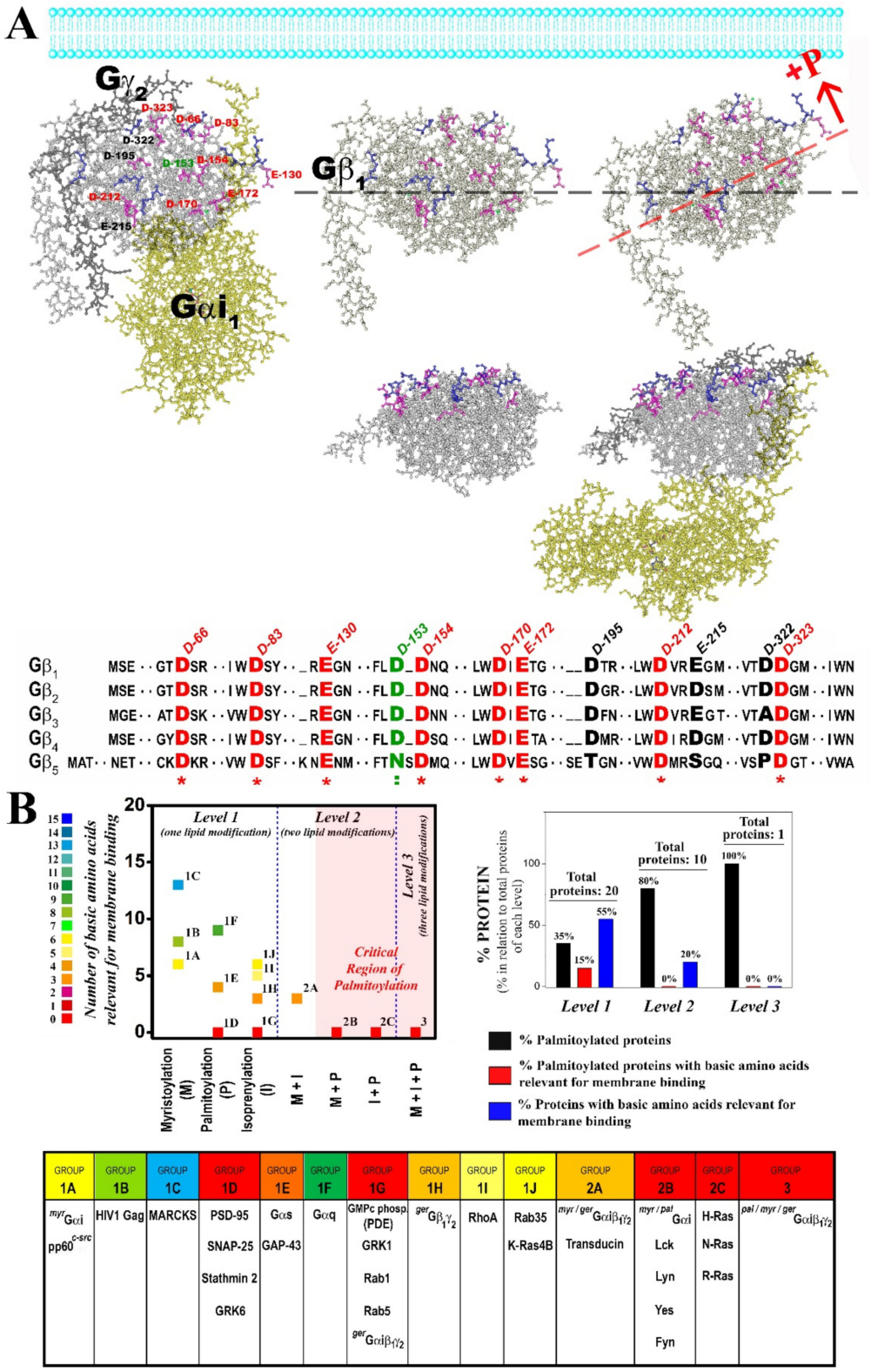

Figure 10. Lipid modifications to G proteins and other peripheral membrane proteins affect their interaction with anionic membrane lipids. (**A**), Possible orientation of Gαi1β1γ2 with respect to the surface of the plasma membrane. The incorporation of a palmitoyl moiety (+P) to Gαi1 would induce a conformational switch in the relative position of the Gαi1β1γ2 complex with respect to the lipid bilayer plane. Gβ1 would be tilted to the membrane side where the palmitic acid is bound to Gαi1

and consequently, anionic amino acids on the nearby Gβ1 half would approach membrane PS. These changes would drive the electrostatic repulsion experienced by the entire Gαβγ complex in the presence of PS. The anionic amino acids of this Gβ subunit that might be involved in this process are highlighted in a multiple alignment in the figure. Some of these amino acids are totally conserved and are shown in red. The structure shown corresponds to X-ray data coordinates provided by Wall et al. [49] and represented using the Molecular Modeling Database (see Materials and Methods). (**B**), Analysis of the existence of polybasic domains involved in the interaction with membrane lipids in functionally relevant proteins and their relation with the lipidation status of the proteins. Three different levels of complexity are established depending on the number of different lipid modifications the proteins are subjected to. Moreover, the number of basic amino acids involved in the interactions with anionic lipids are determined for each protein analyzed, showing that (a) palmitoylation and isoprenylation have lesser basic amino acid requirements and that (b) this requirement is even lesser in proteins with two or three lipid modifications. Finally, a graph shows the relation between protein palmitoylation and the presence of basic amino acids relevant for membrane binding.

$G\beta_1$ is similar to a barrel with its widest side closest to the most hydrophobic lipidation points of the Gαβ®γ complex according to X-ray diffraction data [49]. On this wider face of the barrel, there is a notable presence of anionic amino acids (Figure 10A). Palmitoylation of $G\alpha i_1$ may expose these negatively charged amino acids to the membrane surface while moving positively charged amino acids away from the membrane surface (Figures 9A,B and 10A). In total, nine aspartates and three glutamates were identified in this region of the $G\beta_1$ protein using the Cn3D 4.3 macromolecular structure viewer. Most of these anionic amino acids on the half of the $G_{\beta 1}$ closest to $G\alpha i_1$ are totally conserved in all the human Gβ subunits (Figure 9A), and they might be the main residues responsible for the repulsion experienced by the palmitoylated heterotrimers. Interestingly, palmitoylation increases $G\alpha i_1$ binding while it reduces $G\alpha i_{1\beta 1\gamma 2}$ binding to biological and PS-rich membranes (Figure 8). Thus, in addition to their divergence in the affinity for nonlamellar regions, G protein monomer and heterotrimer also differ in their affinity for negatively charged membrane regions (Figures 5, 6 and 9A,B,D).

Finally, mutations in the basic $G\gamma_2$ C-terminal amino acids impede the binding of $G\beta_1\gamma_2$-Pal^- $G\alpha i_1$ to PS, also demonstrating the important involvement of the $G\gamma_2$ polybasic domain in Gαiβγ–membrane interactions (Figures 5 and 6). Mutations of Arg-62 (R62G), Lys-64 (K64G) and Lys-65 (K65G) impaired the preferential binding of WT Gβγ-Pal^- $G\alpha i_1$ (C3S $G\alpha i_1$ mutant) to PS membranes but not to non-lamellar prone membranes, consistent with earlier studies describing the prevalent role of lipid modifications in the targeting of Gαβγ to disordered membrane microdomains (L_d microdomains; [24,25,27,36]).

Proteins with one or more lipid modifications and their distinct levels of complexity are shown in Figure 10B. In total, 31 lipidated peripheral membrane proteins involved in cell differentiation and growth, synapsis or vesicle transport were analyzed. They were assigned to three different levels depending on the number of different lipid modifications. In this and previous works, we demonstrated the relevant role of one, two or three different lipid modifications of proteins that are involved in signal transduction [24,35,36]. We also analyzed the involvement of patches of basic amino acids in protein–membrane interactions combined with different lipid modifications and at different levels of complexity (Figure 10B). Our analysis showed that a limited number of palmitoylated proteins (15%) and none of the palmitoylated proteins at levels 2 and 3 interact with anionic lipids through their polybasic domains. Thus, palmitoylation appears to be a general regulator of the interaction between basic amino acids and anionic lipids (i.e., PS, PIPs). From a different point of view, myristoylated proteins have more basic amino acids in the membrane-interacting polybasic domain than palmitoylated and isoprenylated proteins (Figure 10B). Moreover, proteins with double or triple lipidation show less electrostatic interaction requirements than proteins with a unique lipid anchor. This observation is enormously relevant from a biological perspective considering the functional importance of the studied proteins, as it affects their membrane localization and microdomain sublocalization. In this context, we think that this work sheds light on the important modulatory role of the palmitoyl

moiety and other membrane lipids on signal transduction and on other decisive events in cells. Thus, a nonlinear analysis showed an inverse correlation between the number of total C atoms present in the lipid anchors in the seven groups of lipid-modified proteins and the number of positively charged amino acids necessary for membrane binding ($n = 7$, $r = 0.93$; $r^2 = 0.87$; $\chi^2 = 1.54$; Figure 10B). This indicates that although charged amino acids are required for the binding of proteins with no lipid anchors, in proteins with several lipid modifications, these amino acids are involved in membrane nanodomain localization rather than in the binding to membranes. Moreover, the higher the number of lipid modifications in an amphitropic protein, the higher its probability to bear a palmitoyl moiety (Figure 10), possibly due to the mobility among different microdomains that provides the reversible presence or absence of this lipid modification. However, further studies will be required to determine the precise roles of all these protein structures and membrane lipid compositions in protein–lipid interactions, cell signaling, pathophysiological processes and melitherapy.

Consequently, we propose here a different model for the interaction between G proteins and biological membranes based on the present and previous results [23,24,35]. According to this model, palmitoylated-myristoylated-geranylgeranylated $G\alpha i_1\beta_1\gamma_2$ heterotrimers would interact with the corresponding GPCRs in anionic lipid-poor and PE-rich membrane microdomains with a high non-lamellar propensity (Figure 9D). This fully lipidated G protein heterotrimer is bound to the GPCR and activated upon ligand binding to the receptor. Then, the GDP associated with $G\alpha i_1$ is exchanged for GTP and the doubly acylated (myristoylated and palmitoylated) $G\alpha i_1$ protein dissociates from the $G\beta_1\gamma_2$ dimer. The turnover of the palmitic acid bound to $G\alpha i_1$ is fast and consequently, the palmitoyl moiety is removed from its N-terminal end [52]. The non-palmitoylated $G\alpha i_1$ protein has a higher affinity for PS-rich raft-like membrane microdomains, where it can inhibit adenylyl cyclase. The migration of the de-palmitoylated monomer toward microdomains with a high density of negative charge is dependent on the basic amino acids situated on the same side of its N-terminal α helix (Figure 9A; [35]).

All $G\alpha$ proteins have GTPase activity and are inactivated by the hydrolysis of GTP to GDP. This reaction is promoted by GAPs (GTPase-activating proteins) and in this sense, the lipid environment of the GAP–$G\alpha$ complexes may play a decisive regulator role. In fact, $G\alpha i$ and RGS4 can interact with anionic lipids, and PS has been seen to influence RGS4 activity [35,53,54]. Furthermore, palmitoylation of $G\alpha i_1$ inhibits its response to RGS4 [54]. In general, palmitoylation is a mechanism closely related to the $G\alpha$ activation-deactivation cycle. Thus, palmitoylation of $G\alpha i_1$ would induce a conformational switch on its N-terminal region, and rotation of the N-terminal α helix would move the basic amino acids away from the membrane surface. Consequently, negatively charged and hydrophobic amino acids on the opposite side of the helix would induce the migration of $G\alpha i_1$ from PS-rich raft-like microdomains toward PS-poor raft-like microdomains (Figure 9).

By contrast, the free $G\beta_1\gamma_2$ heterodimer preferentially localizes to PE and PS-rich microdomains where the $G\gamma_2$ C-terminal basic amino acids Arg-62, Lys-64 and Lys-65 would interact directly with PS. A transient helicoidal structure will appear in this C-terminal region of $G\gamma_2$ upon $G\alpha\beta\gamma$ activation and it appears to be essential for its mobilization to specific membrane microdomains (Figure 9F). Arg-62, Lys-65 and the isoprenoid lipid are responsible for the major preference of $G\beta_1\gamma_2$ for non-lamellar prone and negatively charged microdomains, where PS could interact with the three C-terminal basic amino acids of $G\gamma_2$. PS is likely to be found in these microdomains with high non-lamellar propensity, as demonstrated elsewhere [55–57]. The proximity isoprenyl moieties would induce co-operative binding of additional transducer molecules [16,36,43]. Interestingly, G protein isoprenyl and acyl moieties have different effects on membrane lipid structure, which demonstrates the role of membrane proteins in the regulation of the biophysical properties of membranes [36,43]. Moreover, membrane proteins also regulate the membrane (and therefore the cell) shape [58] Thus, two relevant lipids in cell signaling such as PE and PS can either be enriched in certain membrane micro/nanodomains or can co-segregate in biological membranes, where they strongly modulate the localization of signaling pro-

teins [23,24,35,59–61]. $G\beta_1\gamma_2$ heterodimers would be targeted to these microdomains where effector proteins such as GRK2 may also be present. The new $G\beta_1\gamma_2$–GRK2 complex formed as a result would move to a non-lamellar prone GPCR domain where the receptor would be desensitized by GRK [24]. The inactive double acylated $G\alpha i_1$ monomer would be localized to PS-poor raft-like microdomains, potentially signaling platforms where the inactive signal transduction machinery would be concentrated [62]. Thus, a receptor-$G\beta_1\gamma_2$–GRK complex and the palmitoylated $G\alpha i_1$ monomer might converge in these raft-like domains where $G\alpha i_1$ and $G\beta_1\gamma_2$ could re-associate to form a pre-active G protein heterotrimer and commence the G protein cycle again. Given the diversity of lipid modifications and polybasic domain amino acid sequences of the different G protein subunits known, it would be expected that their cellular localizations would be slightly different along their activity cycle and monomer/oligomer states and combinations.

5. Conclusions

Here, we revealed important details about the basic mechanisms involved in the G protein–membrane interactions and how they influence the localization of the different physiological forms of these signal transducers: $G\alpha$ monomers, $G\beta\gamma$ dimers and $G\alpha\beta\gamma$ heterotrimers. Our study in part explains how the different G protein forms localize to different membrane microdomains, a critical step to establish the physical protein–protein interactions required for signal propagation [63]. The structural features of each G protein subunit (hydrophobicity, charged amino acids and their positions, lipid modifications), the membrane lipid composition and structure (surface charge, lipid order, nonlamellar propensity) and the reversibility of $G\alpha$ protein acylation are crucial to orchestrate protein–lipid and protein–protein interactions. As GPCR signaling constitutes a major drug discovery target, the present study may be decisive for the rational design of new drugs [38]. Similarly, recent studies show that G protein-coupled receptors have predictable cholesterol binding sites without a consensus motif, which might have regulatory roles and be relevant for the development of therapies [64]. Indeed, this new knowledge has been used to develop new therapeutic strategies based on the use of synthetic lipids, termed membrane lipid therapy or melitherapy, some of which are currently undergoing clinical trials or are in the earlier stages of pharmaceutical development [38,44,47,65–75]. Finally, the present study in part explains the similarities and differences in the binding preference, kinetics and localization of different G protein subunits previously detected [76].

Supplementary Materials: The following supporting information can be downloaded at: https://www.mdpi.com/article/10.3390/biomedicines11020557/s1 Figure S1. Example of immunoblotting analysis of mutant $G\gamma_2$ subunits overexpressed in Sf9 cells. Left panel, Immunoblotting showing expression of K64G $G\gamma_2$ subunit expressed in Sf9 cells, which were infected with Baculovirus containing the G protein subunit cDNA (I, infected) or cells which were not infected with it (C, Control). Right panel, Immunoblotting showing the expression of the double $G\gamma_2$ subunit mutants C68S-K64G and C68S-K65G (I) and their corresponding controls (C). Figure S2. Purification of WT and mutant $G\beta_1\gamma_2$ dimers overexpressed in Sf9 cells. The different G protein dimers were purified as described in the Materials and Methods Section 2. Those liquid chromatography fractions rich in each mutant are shown with an asterisk after analysis on 10% polyacrylamide SDS-PAGE gels. Figure S3. Analysis of purified $G\beta_1\gamma_2$ dimers on nondenaturing gels. Proteins were fractioned on non-denaturing 8% polyacrylamide gels and detected with an anti- $G\gamma_2$ antibody (upper panel) or anti- $G\beta_1$ antibody (lower panel). R62: R62G; K64: K64G; K65: K65G; C68: C68S. Figure S4. Binding of $G\beta_1$ and $G\gamma_2$ monomers to Sf9 cell membranes. The graphs show the membrane-to-cytosol distribution of these G protein subunits, which were expressed independently in Sf9 cells. A, The $G\gamma_2$ wild-type and K64G subunits show a membrane (P, pellet) preference, whereas loss of the geranylgeranyl moiety (C68) induces a dramatic increase in the presence of this protein in the cytosol (SN, supernatant). B, The $G\beta_1$ subunit showed a preference for membranes. No $G\gamma_2$ subunit mutants were used in the present study. P: pellet; SN: supernatant. Figure S5. $G\beta_1\gamma_2$ dimer binding to Sf9 cell membranes. Distribution of wild-type (solid bars) and mutant (open bars) $G\beta_1\gamma_2$ heterodimers to Sf9 membranes (P, pellet) and soluble (SN, supernatant) fractions as determined with the anti-$G\gamma_2$ (A) and -$G\beta_1$ (B) antibodies.

These two G protein subunits were co-expressed in Sf9 cells. The observed differences were most likely due to differences in antibody affinities and/or differential expression of these proteins in insect cells. These differences were reduced by the subsequent chromatographic purification process carried out before model-membrane binding experiments. Figure S6. Analysis of purified $G\alpha_i\beta_i\gamma_2$ trimers on nondenaturing gels. Proteins were fractioned on non-denaturing 8% polyacrylamide gels and detected with an anti- $G\alpha_{i1}$ antibody (A) or anti-$G\beta_1$ antibody (B). Panel C shows the recovery of different G protein heterotrimers after affinity chromatography. For other details, see text. C68: C68S; RKK: R62G-K64G-K65G. Figure S7. Effect of the $G\beta_1\gamma_2$ dimer on the binding of wild type and mutant $G\alpha_{i1}\beta_1\gamma_2$ trimers to Sf9 membranes. The binding of the wild-type and mutated $G\alpha_{i1}$ subunit was measured in Sf9 cell membranes in the presence (due to co-expression) or absence of wild-type $G\beta_1\gamma_2$ dimers. A, Effect of the $G\beta_1\gamma_2$-dimer on the binding of $G\alpha_{i1}$ subunits to Sf9 cell membranes as a function of the amount of $G\gamma_2$ subunit measured. B, Effect of the $G\beta_1\gamma_2$-dimer on the binding of $G\alpha_{i1}$ subunits to Sf9 cell membranes as a function of the amount of $G\beta_1$ subunit measured. C, Effect of the $G\beta_1\gamma_2$-dimer on the binding of non-myristoylated (Myr-Gα), non-palmitoylated (Pal-Gα) or diacylated (myristoylated and palmitoylated, WT Gα) $G\alpha_1$ protein with respect to the binding of the $G\alpha_1$ protein alone. Figure S8. Effect of $G\alpha_1$ mutations on the binding of $G\alpha_{i1}\beta_1\gamma_2$ heterotrimers to Sf9 membranes. The levels of the wild-type and mutated $G\alpha_{i1}$ subunits were measured in Sf9 cell membranes (P, pellet) and cytosol (SN, supernatant) from cells that co-expressed the wild-type $G\beta_1\gamma_2$ heterodimer. Data represent mean ± S.E.M. values; * $p < 0.05$ with respect to WT $G\alpha_{i1}$; ** $p < 0.01$ with respect to WT $G\alpha_{i1}$; # $p < 0.05$ between Myr- (G2A mutant) $G\alpha_{i1}$ and Pal- $G\alpha_{i1}$. Figure S9. Effect of mutations on $G\gamma_2$ on the binding of $G\alpha_{i1}\beta_1\gamma_2$ heterotrimers to Sf9 membranes. The levels of G protein heterotrimers with the wild-type and mutated $G\gamma_2$ subunits were measured in Sf9 cell membranes (P, pellet) and cytosol (SN, supernatant) from cells that co-expressed the alpha, beta and gamma subunits indicated. Data represent mean ± S.E.M. values: * $p < 0.05$, *** $p < 0.001$ with respect to WT $G\gamma_2$; ϕ $p < 0.05$ between $G\gamma_2$ C68S K64G and $G\gamma_2$ C68S K65G; # $p < 0.05$ between $G\gamma_2$ C68S and $G\gamma_2$ C68S K64G. Figure S10. Representative immunoblots of G protein-membrane binding experiments. Wild type and mutant G proteins were incubated with preformed model membranes (liposomes) containing the different lipids indicated in the Materials and Methods Section 2. Bound and free G proteins were separated by ultracentrifugation and samples from the pellet and supernatant were fractioned by electrophoresis (SDS-PAGE). G protein binding to membranes was quantified by immunoblotting using specific antibodies and known amounts of a G protein standard.

Author Contributions: R.Á. carried out the experiments, analyzed the data, carried out the statistical analysis and prepared the graphs and P.V.E. designed the study, obtained funding, analyzed and interpreted data and wrote the manuscript. All authors have read and agreed to the published version of the manuscript.

Funding: This work was supported by the European Commission (H2020 Framework Programme Project CLINGLIO 755179), by the Marathon Foundation (Grant MF2018-pve), by Direcció General de Recerca Desenvolupament i Innovació del Govern de les Illes Balears (co-funded by the European Social Fund: ES01/TCAI/24-2018 and PROCOE/5/2017 projects) and by Ministerio de Ciencia e Innovación del Gobierno de España (Retos Colaboración 2019—GLIOPROG561).

Institutional Review Board Statement: Not applicable.

Informed Consent Statement: Not applicable.

Data Availability Statement: Not applicable.

Acknowledgments: The coordinates for the structure of the $G\alpha_1\beta_1\gamma_2$ heterotrimer with GDP were obtained from the Molecular Modeling Database (MMDB identifier number 49238).

Conflicts of Interest: The authors declare no conflict of interest.

References

1. Escribá, P.V.; Wedegaertner, P.B.; Goñi, F.M.; Vögler, O. Lipid-protein interactions in GPCR-associated signaling. *Biochim. Biophys. Acta* **2007**, *1768*, 836–852. [CrossRef]
2. Vögler, O.; Barceló, J.M.; Ribas, C.; Escribá, P.V. Membrane interactions of G proteins and other related proteins. *Biochim. Biophys. Acta* **2008**, *1778*, 1640–1652. [CrossRef]
3. Dupré, D.J.; Robitaille, M.; Rebois, R.V.; Hébert, T.E. The Role of Gβγ Subunits in the Organization, Assembly, and Function of GPCR Signaling Complexes. *Annu. Rev. Pharmacol. Toxicol.* **2009**, *49*, 31–56. [CrossRef] [PubMed]

4. Syrovatkina, V.; Alegre, K.O.; Dey, R.; Huang, X.Y. Regulation, signaling, and physiological functions of G-Proteins. *J. Mol. Biol.* **2016**, *428*, 3850–3868. [CrossRef]
5. López, D.J.; Alvarez, R.; Escribá, P.V. Lipid-protein interactions in G protein signal transduction. In *G Protein-Coupled Receptors: From Structure to Function*, 1st ed.; RSC Publishing: Cambridge, UK, 2011; pp. 153–178.
6. Noguera-Salvà, M.A.; Guardiola-Serrano, F.; Martin, M.L.; Marcilla-Etxenike, A.; Bergo, M.O.; Busquets, X.; Escribá, P.V. Role of the C-terminal basic amino acids and the lipid anchor of the $G\gamma_2$ protein in membrane interactions and cell localization. *Biochim. Biophys. Acta* **2017**, *1859*, 1536–1547. [CrossRef]
7. Jones, T.L.; Simonds, W.F.; Merendino, J.J., Jr.; Brann, M.R.; Spiegel, A.M. Myristoylation of an inhibitory GTP-binding protein alpha subunit is essential for its membrane attachment. *Proc. Natl. Acad. Sci. USA* **1990**, *87*, 568–572. [CrossRef]
8. Mumby, S.M.; Casey, P.J.; Gilman, A.G.; Gutowski, S.; Sternweis, P.C. G protein gamma subunits contain a 20-carbon isoprenoid. *Proc. Natl. Acad. Sci. USA* **1990**, *87*, 5873–5877. [CrossRef]
9. Linder, M.E.; Middleton, P.; Hepler, J.R.; Taussig, R.; Gilman, A.G.; Mumby, S.M. Lipid modifications of G proteins: α subunits are palmitoylated. *Proc. Natl. Acad. Sci. USA* **1993**, *90*, 3675–3679. [CrossRef] [PubMed]
10. Alves, I.D.; Lecomte, S. Study of G-Protein Coupled Receptor Signaling in Membrane Environment by Plasmon Waveguide Resonance. *Acc. Chem. Res.* **2019**, *52*, 1059–1067. [CrossRef] [PubMed]
11. Liu, S.; Luttrell, L.M.; Premont, R.T.; Rockey, D.C. β-Arrestin is a critical component of the GPCR-eNos signalosome. *Proc. Natl. Acad. Sci. USA* **2020**, *117*, 11483–11492. [CrossRef]
12. Hanyaloglu, A.C. Advances in membrane trafficking and endosomal signaling of G protein-coupled receptors. *Int. Rev. Cell Mol. Biol.* **2018**, *339*, 93–131.
13. Zhang, H.; Ping, H.; Zhou, Q.; Lu, Y.; Lu, B. The potential oncogenic and MLN4924-resistant effects of CSN5 on cervical cancer cells. *Cancer Cell Int.* **2021**, *21*, 369. [CrossRef]
14. Singer, S.J.; Nicolson, G. The fluid mosaic model of the structure of cell membranes. *Science* **1972**, *175*, 720–731. [CrossRef] [PubMed]
15. Vereb, G.; Szollosi, J.; Matko, J.; Nagy, P.; Farkas, T.; Vigh, L.; Matyus, L.; Waldmann, T.A.; Damjanovich, S. Dynamic, yet structured: The cell membrane three decades after the Singer-Nicolson model. *Proc. Natl. Acad. Sci. USA* **2003**, *100*, 8053–8058. [CrossRef] [PubMed]
16. Escribá, P.V. Membrane-lipid therapy: A new approach in molecular medicine. *Trends Mol. Med.* **2006**, *12*, 34–43. [CrossRef] [PubMed]
17. Escribá, P.V.; González-Ros, J.M.; Goñi, F.M.; Kinnunen, P.K.; Vigh, L.; Sánchez-Magraner, L.; Fernández, A.M.; Busquets, X.; Horváth, I. Membranes: A meeting point for lipids, proteins and therapies. *J. Cell. Mol. Med.* **2008**, *12*, 829–875. [CrossRef]
18. Lingwood, D.; Simons, K. Lipid rafts as a membrane-organizing principle. *Science* **2010**, *327*, 46–50. [CrossRef]
19. Nicolson, G.L. The fluid-mosaic model of membrane structure: Still relevant to understanding the structure, function and dynamics of biological membranes after more than 40 years. *Biochim. Biophys. Acta* **2014**, *1838*, 1451–1466. [CrossRef]
20. Torres, M.; Rosselló, C.A.; Fernáncez-García, P.; Lladó, V.; Kakhlon, O.; Escribá, P.V. The implications for cells of the lipid switches driven by protein-membrane interactions and the development of membrane lipid therapy. *Int. J. Mol. Sci.* **2019**, *21*, 2322. [CrossRef]
21. Israelachvili, J.N.; Marcelja, S.; Horn, R.G. Physical principles of membrane organisation. *Quart. Rev. Biophys.* **1980**, *13*, 121–200. [CrossRef]
22. Escribá, P.V.; Sastre, M.; García-Sevilla, J.A. Disruption of cellular signaling pathways by daunomycin through destabilization of nonlamellar membrane structures. *Proc. Natl. Acad. Sci. USA* **1995**, *92*, 7595–7599. [CrossRef] [PubMed]
23. Escribá, P.V.; Ozaita, A.; Ribas, C.; Miralles, A.; Fodor, E.; Farkas, T.; García-Sevilla, J.A. Role of lipid polymorphism in G protein-membrane interactions: Nonlamellar-prone phospholipids and peripheral protein binding to membranes. *Proc. Natl. Acad. Sci. USA* **1997**, *94*, 11375–11380. [CrossRef] [PubMed]
24. Vögler, O.; Casas, J.; Capó, D.; Nagy, T.; Borchert, G.; Martorell, G.; Escribá, P.V. The Gβγ dimer drives the interaction of heterotrimeric Gi proteins with nonlamellar membrane structures. *J. Biol. Chem.* **2004**, *279*, 36540–36545. [CrossRef]
25. Melkonian, K.A.; Ostermeyer, A.G.; Chen, J.Z.; Roth, M.G.; Brown, D.A. Role of lipid modifications in targeting proteins to detergent-resistant membrane rafts. Many raft proteins are acylated, while few are prenylated. *J. Biol. Chem.* **1999**, *274*, 3910–3917. [CrossRef]
26. Lu, X.; Sicard, R.; Jiang, X.; Stockus, J.N.; McNamara, G.; Abdulreda, M.; Moy, V.T.; Landgraf, R.; Lossos, I.S. HGAL localization to cell membrane regulates B-cell receptor signaling. *Blood* **2015**, *125*, 649–657. [CrossRef] [PubMed]
27. Moffett, S.; Brown, D.A.; Linder, M.E. Lipid-dependent targeting of G proteins into rafts. *J. Biol. Chem.* **2000**, *275*, 2191–2198. [CrossRef]
28. Zhou, Y.; Prakash, P.S.; Liang, H.; Gorfe, A.A.; Hancock, J.F. The KRAS and other prenylated polybasic domain membrane anchors recognize phosphatydilserine acyl chain structure. *Proc. Natl. Acad. Sci. USA* **2021**, *118*, e2014605118. [CrossRef]
29. Koklič, T.; Hrovat, A.; Guixà-González, R.; Rodríguez-Espigares, I.; Navio, D.; Frangež, R.; Uršič, M.; Kubale, V.; Plemenitaš, A.; Selent, J.; et al. Electron paramagnetic resonance gives evidence for the presence of Type 1 Gonadotropin-Releasing Hormone Receptor (GnRH-R) in subdomains of lipid rafts. *Molecules* **2021**, *26*, 973. [CrossRef]

30. Eggeling, C.; Ringemann, C.; Medda, R.; Schwarzmann, G.; Sandhoff, K.; Polyakova, S.; Belov, V.N.; Hein, B.; von Middendorff, C.; Schönle, A.; et al. Direct observation of the nanoscale dynamic of membrane lipids in a living cell. *Nature* **2009**, *457*, 1159–1162. [CrossRef]
31. Sot, J.; Ibarguren, M.; Busto, J.V.; Montes, L.R.; Goñi, F.M.; Alonso, A. Cholesterol displacement by ceramide in sphingomyelin-containing liquid-ordered domains, and generation of gel regions in giant lipidic vesicles. *FEBS Lett.* **2008**, *582*, 3230–3236. [CrossRef]
32. Rothman, J.E.; Lenard, J. Membrane asymmetry. *Science* **1977**, *195*, 743–753. [CrossRef] [PubMed]
33. Hessel, E.; Heck, M.; Müller, P.; Herrmann, A.; Hofmann, K.P. Signal Transduction in the Visual Cascade Involves Specific Lipid-Protein Interactions. *J. Biol. Chem.* **2003**, *278*, 22853–22860. [CrossRef] [PubMed]
34. Zhou, Y.; Wong, C.; Cho, K.; van der Hoeven, D.; Liang, H.; Thakur, D.P.; Luo, J.; Babic, M.; Zinsmaier, K.E.; Zhu, M.X.; et al. Membrane potential modulates plasma membrane phospholipid dynamics and K-Ras signaling. *Science* **2015**, *349*, 873–876. [CrossRef] [PubMed]
35. Alvarez, R.; López, D.J.; Casas, J.; Lladó, V.; Higuera, M.; Nagy, T.; Barceló, M.; Busquets, X.; Escribá, P.V. G protein-membrane interactions I: Gαi_1 myristoyl and palmitoyl modifications in protein-lipid protein–lipid interactions and its implications in membrane microdomain localization. *Biochim. Biophys. Acta* **2015**, *1851*, 1511–1520. [CrossRef]
36. Casas, J.; Ibarguren, M.; Álvarez, R.; Terés, S.; Lladó, V.; Piotto, S.; Concilio, S.; Busquets, X.; López, D.J.; Escribá, P.V. G protein-membrane interactions II: Effect of G protein-linked lipids on membrane structure and G protein-membrane interactions. *Biochim. Biophys. Acta* **2017**, *1859*, 1526–1535. [CrossRef]
37. Damian, M.; Louet, M.; Gomes, A.A.S.; M'Kadmi, C.; Denoyelle, S.; Cantel, S.; Mary, S.; Bisch, P.M.; Fehrentz, J.-A.; Catoire, L.J.; et al. Allosteric modulation of ghrelin receptor signaling by lipids. *Nat. Commun.* **2021**, *12*, 3938. [CrossRef]
38. Escribá, P.V. Membrane-lipid therapy: A historical perspective of membrane-targeted therapies—From lipid bilayer structure to the pathophysiological regulation of cells. *Biochim. Biophys. Acta* **2017**, *1859*, 1493–1506. [CrossRef]
39. Maldonado, C.; Nguyen, M.-D.; Bauer, P.; Nakamura, S.; Khundmiri, S.; Perez-Abadia, G.; Stowers, H.L.; Wu, W.-J.; Tang, X.-L. Rapid lipid modification of endothelial cell membranes in cardiac ischemia/reperfusion injury: A novel therapeutic strategy to reduce infarct size. *Cardiovasc. Drugs Ther.* **2021**, *35*, 113–123. [CrossRef]
40. Kozasa, T.; Gilman, A.G. Purification of recombinant G proteins from Sf9 cells by hexahistidine tagging of associated subunits. *J. Biol. Chem.* **1995**, *270*, 1734–1741. [CrossRef]
41. García-Sevilla, J.A.; Escribá, P.V.; Ozaita, A.; La Harpe, R.; Walzer, C.; Eytan, A.; Guimón, J. Regulation of immunolabeled α2A-adrenoceptors, Gi coupling proteins, and regulatory receptor kinases in the prefrontal cortex of depressed suicides. *J. Neurochem.* **1999**, *72*, 282–291. [CrossRef]
42. Escribá, P.V.; Sánchez-Domínguez, J.M.; Alemany, R.; Perona, J.S.; Ruiz-Gutierrez, V. Alteration of lipids, G proteins, and PKC in cell membranes of elderly hypertensives. *Hypertension* **2003**, *41*, 176–182. [CrossRef] [PubMed]
43. Barceló, F.; Prades, J.; Encinar, J.A.; Funari, S.S.; Vögler, O.; González-Ros, J.M.; Escribá, P.V. Interaction of the C-terminal region of the Gg protein with model membranes. *Biophys. J.* **2007**, *93*, 2530–2541. [CrossRef]
44. Terés, S.; Barceló-Coblijn, G.; Benet, M.; Alvarez, R.; Bressani, R.; Halver, J.E.; Escribá, P.V. Oleic acid content is responsible for the reduction in blood pressure induced by olive oil. *Proc. Natl. Acad. Sci. USA* **2008**, *105*, 13811–13816. [CrossRef] [PubMed]
45. Ibarguren, M.; López, D.J.; Encinar, J.A.; González-Ros, J.M.; Busquets, X.; Escribá, P.V. Partitioning of liquid-ordered/liquid-disordered membrane microdomains induced by the fluidifying effect of 2-hydroxylated fatty acid derivatives. *Biochim. Biophys. Acta* **2013**, *1828*, 2553–2563. [CrossRef] [PubMed]
46. Ibarguren, M.; López, D.J.; Escribá, P.V. The effect of natural and synthetic fatty acids on membrane structure, microdomain organization, cellular functions and human health. *Biochim. Biophys. Acta* **2014**, *1838*, 1518–1528. [CrossRef]
47. Terés, S.; Lladó, V.; Higuera, M.; Barceló-Coblijn, G.; Martin, M.L.; Noguera-Salvà, M.A.; Marcilla-Etxenike, A.; García-Verdugo, J.M.; Soriano-Navarro, M.; Saus, C.; et al. 2-Hydroxyoleate, a nontoxic membrane binding anticancer drug, induces glioma cell differentiation and autophagy. *Proc. Natl. Acad. Sci. USA* **2012**, *109*, 8489–8494. [CrossRef] [PubMed]
48. Escribá, P.V.; Busquets, X.; Inokuchi, J.-I.; Balogh, G.; Török, Z.; Horváth, I.; Harwood, J.L.; Vígh, L. Membrane lipid therapy: Modulation of the cell membrane composition and structure as a molecular base for drug discovery and new disease treatment. *Prog. Lipid Res.* **2015**, *59*, 38–53. [CrossRef]
49. Wall, M.A.; Coleman, D.E.; Lee, E.; Iñiguez-Lluhi, J.A.; Posner, B.A.; Gilman, A.G.; Sprang, S.R. The Structure of the G Protein Heterotrimer Giα1β1γ2. *Cell* **1995**, *83*, 1047–1058. [CrossRef]
50. Lambright, D.G.; Sondek, J.; Bohm, A.; Skiba, N.P.; Hamm, H.E.; Sigler, P.B. The 2.0 A crystal structure of a heterotrimeric G protein. *Nature* **1996**, *379*, 311–319. [CrossRef]
51. van Keulen, S.C.; Rothlisberger, U. Exploring the inhibition mechanism of adenylyl cyclase type 5 by n-terminal myristoylated Gαi1. *PLoS Comput. Biol.* **2017**, *13*, e1005673. [CrossRef]
52. Degtyarev, M.Y.; Spiegel, A.M.; Jones, T.L.Z. Palmitoylation of a G Protein αi Subunit Requires Membrane Localization Not Myristoylation. *J. Biol. Chem.* **1994**, *269*, 30898–30903. [CrossRef]
53. Bernstein, L.S.; Grillo, A.A.; Loranger, S.S.; Linder, M.E. RGS4 binds to membranes through an amphipathic alpha-helix. *J. Biol. Chem.* **2000**, *275*, 18520–18526. [CrossRef]
54. Tu, Y.; Woodson, J.; Ross, E.M. Binding of regulator of G protein signaling (RGS) proteins to phospholipid bilayers. Contribution of location and/or orientation to GTPase-activating protein activity. *J. Biol. Chem.* **2001**, *276*, 20160–20166. [CrossRef] [PubMed]

55. Hope, M.J.; Cullis, P.R. The bilayer stability of inner monolayer lipids from the human erythrocyte. *FEBS Lett.* **1979**, *107*, 323–326. [CrossRef] [PubMed]
56. Kirk, G.L.; Gruner, S.M.; Stein, D.L. A Thermodynamic Model of the Lamellar to Inverse Hexagonal Phase Transition of Lipid Membrane-Water Systems. *Biochemistry* **1984**, *23*, 1093–1102. [CrossRef]
57. Matsuzaki, K.; Sugishita, K.; Ishibe, N.; Ueha, M.; Nakata, S.; Miyajima, K.; Epand, R.M. Relationship of membrane curvature to the formation of pores by magainin 2. *Biochemistry* **1998**, *37*, 11856–11863. [CrossRef] [PubMed]
58. Liese, S.; Carlson, A. Membrane shape remodeling by protein crowding. *Biophys. J.* **2021**, *120*, 2482–2489. [CrossRef] [PubMed]
59. Hirama, T.; Das, R.; Yang, Y.; Ferguson, C.; Won, A.; Yip, C.M.; Kay, J.G.; Grinstein, S.; Parton, R.G.; Fairn, G.D. Phosphatidylserine dictates the assembly and dynamics of caveolae in the plasma membrane. *J. Biol. Chem.* **2017**, *292*, 14292–14307. [CrossRef]
60. Guyot, C.; Stieger, B. Interaction of bile salts with rat canalicular membrane vesicles: Evidence for bile salt resistant microdomains. *J. Hepatol.* **2011**, *55*, 1368–1376. [CrossRef]
61. Allender, D.W.; Giang, H.; Schick, M. Model plasma mebrane exhibits a microemulsion in both leaves providing foundation for rafts. *Biophys. J.* **2020**, *118*, 1019–1031. [CrossRef]
62. Huang, C.; Hepler, J.R.; Chen, L.T.; Gilman, A.G.; Anderson, R.G.; Mumby, S.M. Organization of G proteins and adenylyl cyclase at the plasma membrane. *Mol. Biol. Cell* **1997**, *8*, 2365–2378. [CrossRef]
63. Sungkaworn, T.; Jobin, M.-L.; Burnecki, K.; Weron, A.; Lohse, M.J.; Calebiro, D. Single-molecule imaging reveals receptor-G protein interactions at cell surface hot spots. *Nature* **2017**, *550*, 543–547. [CrossRef] [PubMed]
64. Taghon, G.J.; Rowe, J.B.; Kapolka, N.J.; Isom, D.G. Predictable cholesterol binding sites in GPCRs lack consensus motifs. *Structure* **2021**, *29*, 499–506. [CrossRef] [PubMed]
65. Alemany, R.; Terés, S.; Baamonde, C.; Benet, M.; Vögler, O.; Escribá, P.V. 2-Hydroxyoleic acid: A new hypotensive molecule. *Hypertension* **2004**, *43*, 249–254. [CrossRef]
66. Martínez, J.; Vögler, O.; Casas, J.; Barceló, F.; Alemany, R.; Prades, J.; Nagy, T.; Baamonde, C.; Kasprzyk, P.G.; Terés, S.; et al. Membrane structure modulation, protein kinase C alpha activation, and anticancer activity of minerval. *Mol. Pharmacol.* **2005**, *67*, 531–540. [CrossRef]
67. Lladó, V.; Terés, S.; Higuera, M.; Alvarez, R.; Noguera-Salva, M.A.; Halver, J.E.; Escribá, P.V.; Busquets, X. Pivotal role of dihydrofolate reductase knockdown in the anticancer activity of 2-hydroxyoleic acid. *Proc. Natl. Acad. Sci. USA* **2009**, *106*, 13754–13758. [CrossRef] [PubMed]
68. Lopez, D.H.; Fiol-deRoque, M.A.; Noguera-Salvà, M.A.; Terés, S.; Campana, F.; Piotto, S.; Castro, J.A.; Mohaibes, R.J.; Escribá, P.V.; Busquets, X. 2-Hydroxy arachidonic acid: A new non-steroidal anti-inflammatory drug. *PLoS ONE* **2013**, *8*, e72052. [CrossRef]
69. Fiol-deRoque, M.A.; Gutierrez-Lanza, R.; Terés, S.; Torres, M.; Barceló, P.; Rial, R.V.; Verkhratsky, A.; Escribá, P.V.; Busquets, X.; Rodríguez, J.J. Cognitive recovery and restoration of cell proliferation in the dentate gyrus in the 5XFAD transgenic mice model of Alzheimer's disease following 2-hydroxy-DHA treatment. *Biogerontology* **2013**, *14*, 763–775. [CrossRef]
70. Torres, M.; Price, S.L.; Fiol-Deroque, M.A.; Marcilla-Etxenike, A.; Ahyayauch, H.; Barceló-Coblijn, G.; Terés, S.; Katsouri, L.; Ordinas, M.; López, D.J.; et al. Membrane lipid modifications and therapeutic effects mediated by hydroxydocosahexaenoic acid on Alzheimer's disease. *Biochim. Biophys. Acta* **2014**, *1838*, 1680–1692. [CrossRef]
71. Lladó, V.; López, D.J.; Ibarguren, M.; Alonso, M.; Soriano, J.B.; Escribá, P.V.; Busquets, X. Regulation of the cancer cell membrane lipid composition by NaCHOleate: Effects on cell signaling and therapeutical relevance in glioma. *Biochim. Biophys. Acta* **2014**, *1838*, 1619–1627. [CrossRef]
72. Guardiola-Serrano, F.; Beteta-Göbel, R.; Rodríguez-Lorca, R.; Ibarguren, M.; López, D.J.; Terés, S.; Alvarez, R.; Alonso-Sande, M.; Busquets, X.; Escribá, P.V. The Novel Anticancer Drug Hydroxytriolein Inhibits Lung Cancer Cell Proliferation via a Protein Kinase Cα- and Extracellular Signal-Regulated Kinase 1/2-Dependent Mechanism. *J. Pharmacol. Exp. Ther.* **2015**, *354*, 213–224. [CrossRef] [PubMed]
73. Torres, M.; Busquets, X.; Escribá, P.V. Brain Lipids in the Pathophysiology and Treatment of Alzheimer's Disease. In *Update on Dementia*; Moretti, D.V., Ed.; InTech Open: London, UK, 2016; Volume 1, pp. 127–167.
74. Alvarez, R.; Casas, J.; López, D.J.; Ibarguren, M.; Suari-Rivera, A.; Terés, S.; Guardiola-Serrano, F.; Lossos, A.; Busquets, X.; Kakhlon, O.; et al. Triacylglycerol mimetics regulate membrane interactions of glycogen branching enzyme: Implications for therapy. *J. Lipid Res.* **2017**, *58*, 1598–1612. [CrossRef] [PubMed]
75. Vögler, O.; López-Bellan, A.; Alemany, R.; Tofé, S.; González, M.; Quevedo, J.; Pereg, V.; Barceló, F.; Escriba, P.V. Structure-effect relation of C18 long-chain fatty acids in the reduction of body weight in rats. *Int. J. Obes.* **2008**, *32*, 464–473. [CrossRef] [PubMed]
76. O'Neill, P.R.; Karunarathne, W.K.A.; Kalyanaraman, V.; Silvius, J.R.; Gautam, N. G-protein signaling leverages subunit-dependent membrane affinity to differentially control bg translocation to intracellular membranes. *Proc. Natl. Acad. Sci. USA* **2012**, *109*, E3568–E3577. [CrossRef]